Technical Letter Report
TLR-RES/DE/CIB-2021-06

Technical Assistance to Review American Society of Mechanical Engineer's Boiler and Pressure Vessel Code Case and Licensee Relief Requests for Carbon Fiber Repairs

Task-3: Mockup Testing and Physical Evaluation of Proposed Carbon Fiber Reinforced Polymer Repair

Technical Letter Report

M. Uddin, S. Pothana, F. Orth, Y. Hioe
P. Krishnaswamy

Engineering Mechanics Corporation of Columbus (Emc^2)
3518 Riverside Drive - Suite 202
Columbus, OH 43221-1735

Project Manager:
L. Smith
U.S. Nuclear Regulatory Commission
Office of Nuclear Regulatory Research

2021

DISCLAIMER: This report does not contain or imply legally binding requirements. Nor does this report establish or modify any regulatory guidance or positions of the U.S. Nuclear Regulatory Commission and is not binding on the Commission.

EXECUTIVE SUMMARY

The use of Carbon Fiber Reinforced Polymer (CFRP) composites in the nuclear industry is very limited and has not been used for nuclear safety related applications until recently. In 2019, the ASME Boiler and Pressure Vessel Code (BPVC) Committee approved a new Code Case N-871 for Class 2 and 3 safety-related piping using CFRP for Service Levels A, B, C, and D for a service life of 50 years. However, the US Nuclear Regulatory Commission (NRC) has not as yet approved this Code Case for use in commercial nuclear power plants. This Code Case provides guidance for repairing degraded areas of pipe with a full-circumferential application of CFRP on the internal surface without taking any credit for the remaining structural strength of the host pipe.

In the ASME BPV Code Case N-871 (CC N-871), two alternative design methodologies are provided for designing CFRP repairs of safety related piping – Allowable Stress Design (ASD), and Load and Resistance Factor Design (LRFD) methods. Both methods are reviewed in detail in this report. While the fundamental design philosophy in both design methods vary, the factor of safety for allowable stress values are incorporated and applied so as to account for various uncertainties arising from factors such as: applied loads, manufacturing procedures affecting the properties of CFRP materials, installation conditions such as curing and post-curing temperatures, quality control such as allowable misalignment angle, and material property degradation over time such as environmental exposure and creep.

In this project, the available margin in Class 2 and 3 degraded piping repaired by CFRP per ASME BPV CC N-871 has been evaluated by conducting the following sets of experiments at Emc2's laboratory:

- A series of confirmatory *coupon tests* to determine the effect of the strength reduction factors for CFRP noted above
- *Small-scale hydrostatic watertightness tests* used by the industry to confirm the quality of CFRP repair procedures and estimate the failure pressure at leak, and
- One *full-scale confirmatory hydrostatic test* of a pipe specimen with an artificial defect (12-inch x 24-inch hole) to simulate degradation of the pipe designed to operate at 84 psi during service – which was repaired with CFRP per CC N-871. This specimen was tested at room temperature (72 F) to failure under internal hydrostatic pressure loading. The available margin under this short-term hydrostatic loading was then determined using the pressure at which leakage first occurred during this test.

ACKNOWLEDGEMENT

This work was supported by the U.S. Nuclear Regulatory Commission through the Component Integrity Engineering Branch of the Division of Engineering in the Office of Nuclear Regulatory Research under Contract NRC-HQ-25-14-E-0004; Task UN 7 from NUMARK,

We would like to thank Dr. Laura Smith of NRC-RES, the Contracting Officer's Representative (COR) and Dr. Chakrapani Basavaraju of NRC-NRR, the alternative COR of this project for their valuable comments and suggestions as well as Ms. Carol Nove, Dr. Patrick Raynaud, and Dr. Raj Iyengar of NRC-RES and Mr. Jay Collins, Dr. Seung Min of NRC-NRR.

Table of Contents

EXECUTIVE SUMMARY ii
ACKNOWLEDGEMENT iv
1. BACKGROUND 1
1.1 Design Methodologies for CFRP Repair 1
1.1.1 Allowable Stress Design (ASD) Method 1
1.1.2 Load and Resistance Factor Design (LRFD) Method 2
1.1.3 Effective Factor of Safety in ASD and LRFD Methods 2
1.2 Strength Reduction Phenomena in CFRP Repair System 3
1.2.1 Variation in statistical analysis of ultimate strength – 4
1.2.2 Effect of multi-ply laminate 4
1.2.3 Effect of misalignment angle 5
1.2.4 Time effect factor due to sustained loading 5
1.2.5 Materials adjustment factors due to harsh environmental exposure 6
1.2.6 Effect of temperature 7
1.3 Recent Update on Code Case N-871 7
2. OBJECTIVES AND APPROACH 7
3. DETERMINATION OF VARIOUS STRENGTH REDUCTION FACTORS 8
3.1 Variation in Statistical Analysis of Ultimate Strength 8
3.2 Strength determination for Multi-Ply Laminates 10
3.3 Effect of Misalignment Angle 14
3.4 Ongoing Investigation of Remaining Strength Reduction Factors 16
3.4.1 Long-Term Material Degradation Factors 16
3.4.2 Effect of Temperatures 17
3.5 Summary of Various Strength Reduction Factors 17
4. BOND STRENGTHS AT TERMINAL ENDS 18
4.1 Lap Shear Strength 19
4.2 Pull-off Strength 20
5. EFFECTIVE FACTOR OF SAFETY, FS_{eff} FOR CFRP REPAIR SYSTEM 21
5.1 Impact of Results on Current Version of Code Case N-871 23
6. WATERTIGHTNESS TEST 24
7. FULL-SCALE HYDROSTATIC TEST OF THE CFRP REPAIR SYSTEM 26
7.1 The Full-Scale Hydrostatic Test Design 26
7.2 Design Calculation of the CFRP Repair System 29

7.3 Installation of CFRP Repair System 30
7.3.1 Key steps during installation 30
7.3.2 Some other steps during installation 32
7.3.3 Curing and post-curing temperatures during installation 33
7.3.4 Degree of curing and glass transition temperature (T_g) 36
7.3.5 Results of witness panels 38
7.4 Performance of the Hydrostatic Test 38
7.4.1 Hydrostatic test setup and instrumentation 38
7.4.2 Hydrostatic test results 40
7.5 Available Margin in CFRP Repair System 44
7.5.1 Failure modes 44
7.5.2 Effect of long-term use and elevated temperature on the available margin 45
8. SUMMARY 45
9. FUTURE RECOMMENDATIONS ..... **Error! Bookmark not defined.**
REFERENCES 49

List of Figures

Figure 1 Tensile test results for single-ply CFRP laminate 9
Figure 2 Ultimate strength of single-ply CFRP laminate 9
Figure 3 Statistical analyses of single-ply CFRP (C400H) laminate tensile tests 10
Figure 4 Ultimate strength of single and multi-ply CFRP (C200H) laminates tested at SGH and Emc^2 12
Figure 5 Determination of characteristic and basis values of ultimate tensile strengths for 1-ply, 2-ply, 3-ply and 4-ply CFRP (C200H) laminate 13
Figure 6 Schematic of off-axis CFRP tensile specimen 15
Figure 7 Comparison of ultimate strength and modulus of single-ply off-axis and unidirectional CFRP laminates 16
Figure 8 Single and double lap shear test results for GFRP on steel substrates 20
Figure 9 Double lap shear test results for GFRP on steel and aluminum-bronze substrates 20
Figure 10 Pull-off test results for GFRP on steel and aluminum-bronze substrates 21
Figure 11 The watertightness fixture built a Emc^2 25
Figure 12 The watertightness test panels showing matrix cracking after test 25
Figure 13 3D finite element model (half-symmetry) of full-scale pipe with a cut-out and CFRP repair 27
Figure 14 Three flaw dimensions for FE model 27
Figure 15 Hoop and longitudinal stresses in the steel host pipe under 500 psi internal pressure. 28
Figure 16 Shear stresses in adhesive between steel host pipe and CFRP repair under 200 psi internal pressure 28
Figure 17 Hoop strain in CFRP hoop layer under 200 psi internal pressure 29
Figure 18 The test pipe with 12″ × 24″ cut-out before CFRP installation 30
Figure 19 The high-level CFRP repair installation process flow diagram 31
Figure 20 The key steps in CFRP repair installation process 32
Figure 21 Some other steps in CFRP repair installation process 33
Figure 22 Temperature data loggers and thermocouples installed to monitor curing and post-curing temperatures 34
Figure 23 Temperature and relative humidity data from the data loggers over entire period of curing and post-curing 35
Figure 24 Temperature data from thermocouples installed under each layer of CFRP repair system over entire period of curing and post-curing 36
Figure 25 DSC results for three samples collected from CFRP repair system of the test 37
Figure 26 Schematic of the full-scale hydrostatic test setup 38
Figure 27 Photographs showing various steps of the test setup 39
Figure 28 Instrumentation for the full-scale hydrostatic test 40
Figure 29 Pressure versus time data from the full-scale hydrostatic test 41
Figure 30 Onset of initial and final leak during the hydrostatic test 41
Figure 31 Pressure versus bulging during the hydrostatic test 42
Figure 32 Temperature data during the hydrostatic test 43
Figure 33 Strain gage data on host pipe and CFRP during the hydrostatic test 43
Figure 34 River-like matrix cracking on CFRP system inside the pipe after hydrostatic test 44

List of Tables

Table 1 Tensile test results for single-ply laminate 9
Table 2 Characteristic values of ultimate tensile strength for single-ply CFRP (C400H) laminate 10
Table 3 Characteristic and basis values of ultimate tensile strengths for 1-ply, 2-ply, 3-ply and 4-ply CFRP (C200H) laminate showing strength reduction for multi-ply laminate..... 13
Table 4 Statistical values of ultimate tensile strengths for 1-ply, 2-ply, 3-ply and 4-ply CFRP (C200H) laminate showing variations in statistical analyses 14
Table 5 Comparison of single-ply off-axis tensile test results with unidirectional CFRP laminate 15
Table 6 List of various strength reduction phenomena for CFRP repair system..... 18
Table 7 Lap shear results for GFRP on steel and aluminum-bronze substrates 19
Table 8 Pull-off test results for GFRP on steel and aluminum-bronze substrates 21
Table 9 Watertightness test results 25
Table 10 The input values for design calculation of the CFRP repair system..... 29
Table 11 Degree of cure and glass transition temperature (T_g) of CFRP repair system..... 37

1. BACKGROUND

Carbon Fiber Reinforced Polymer composites (CFRP) have been used for decades in the aerospace, oil and gas, and transportation industries mainly due to their high strength-to-weight-ratio and excellent corrosion resistance. However, the use of CFRP in the nuclear industry is very limited and had not been used for any nuclear safety related applications until recently. In 2019, the ASME Boiler and Pressure Vessel Code (BPVC) Committee approved new Code Case N-871 for Class 2 and 3 safety-related piping using CFRP for Service Levels A, B, C, and D for a service life of 50 years [1]. However, the US Nuclear Regulatory Commission (NRC) has not as yet approved this Code Case for use in commercial nuclear power plants. Per this Code Case, repairs are designed to be applied using a full-circumferential application of CFRP composite on degraded portions of metallic pipes and fittings without taking any credit for the remaining structural strength of the host pipe.

In 2016, a relief request was submitted to NRC by Surry Nuclear Power Station of the Virginia Electric and Power Company to perform an internal repair of degraded ASME Class 2 and 3 safety related circulating and service water buried piping using CFRP based on the Load and Resistance Factor Design (LRFD) method. This relief request was approved by the NRC and the CFRP repair was subsequently implemented in two pipe systems at Surry [2,3].

The following sections provide the background on the design methodologies for CFRP repair including the various factors that reduce the strength of the CFRP materials which can affect the overall factor of safety of the repair system.

1.1 Design Methodologies for CFRP Repair

In the ASME BPV Code Case N-871, two alternative design methodologies are provided for designing CFRP repair of safety related piping – Allowable Stress Design (ASD), and Load and Resistance Factor Design (LRFD) methods. Even though the ASME BPV Code Case N-871 is currently planning to delete the LRFD method from the design section, it is still relevant to review this method which was used in the 2016 relief request submitted to NRC. While the ASD approach described in the ASME BPV Code Section III [4] is commonly used for nuclear applications, the LRFD approach has never been previously used in nuclear safety-related applications. However, the LRFD method has been used extensively for civil engineering structures for decades [5, 6, 7, 8, 9]. Both design methods have been reviewed in detail for CFRP repair for nuclear Class 2 and Class 3 safety related piping in a paper by the authors of this report [10].

1.1.1 Allowable Stress Design (ASD) Method

The design philosophy of the ASD method requires that the nominal load for any specified service condition not exceed the allowable design stress reduced by a factor of safety. This load includes both normal dead and transient loads and the allowable design stress is based on a material's resistance. The general form for the ASD method is given as

$$Load\ effect \leq \frac{Allowable\ stress}{Factor\ of\ Safety} \qquad (1)$$

In the ASD method, all uncertainties arising from loads, manufacturing, installation, quality control, materials' property degradation are addressed through one variable, the Factor of Safety (*FS*).

1.1.2 Load and Resistance Factor Design (LRFD) Method

In the LRFD method, the design is based on target reliability indices that correspond to probability of failure. The target reliability index is typically set according to a specific application such as $<10^{-6}$ probability of failure for nuclear safety related applications. The LRFD method addresses uncertainties in both material properties and loads by incorporating factors such as load factor and resistance factor, and hence the name LRFD method. In the context of specific applications of CFRP repair of safety related piping, several other factors, such as materials adjustment factors and time effect factors are incorporated in the resistance side of the design equation [9]. The general form for the LRFD method is

$$R_u \leq \phi R_n \qquad (2)$$

where R_n is nominal strength in end-use condition which needs to be determined for the specific material, application, and service life as $R_n = \lambda C R_0$.

Hence, the design equation for LRFD becomes

$$R_u \leq \phi \lambda C R_0 \qquad (3)$$

Where R_u is required strength determined using load factor combination accounting for deviations of the actual load from the nominal load, f is resistance factor corresponding to target reliability index accounting for the variability of material properties due to quality control during manufacturing and installation of CFRP, l is time effect factor corresponding to property degradation due to sustained loading, C is material adjustment factor corresponding to property degradation due to environmental exposure and Ro is the characteristic value of the material properties (discussed in a later section).

1.1.3 Effective Factor of Safety in ASD and LRFD Methods

In this report, the effective factor of safety, FS_{eff} is designated as the difference between the allowable stress (or strength) and the computed stress (or demand) where the allowable stresses (or strengths) are reduced by relevant strength reduction factors in CFRP repair. Some of the strength reduction factors such as λ, C are discussed above in Section 1.1.2 and will be further elaborated (along with other strength reduction factors) in the next section. In this regard, FS_{eff} in the ASD method should be equal to the factor of safety, *FS* (used in Eq. 1) multiplied by all relevant strength reductions factors as defined below.

$$\left(FS_{eff}\right)_{ASD} = \textit{Factor of Safety} \times \textit{All Strength Reduction Factors} \qquad (4)$$

Since the LRFD design method is based on target reliability indices that correspond to 10^{-6} probability of failure and strength reductions factors λ and C are also included in the design equation (Eq. 3), no additional factor of safety is used. Therefore, the design equation is satisfied

when demand to strength ratio is equal to or less than 1.0. The FS_{eff} in the LRFD method can be calculated from the load factor divided by the resistance factor. However, if any other strength reduction factors (except λ and C) are identified in any application, the FS_{eff} in LRFD method should be reduced by those strength reduction factors as shown in Eq. 5.

$$\left(FS_{eff}\right)_{LRFD} = \frac{Load\ factor}{Resistance\ factor} \times Strength\ Reduction\ Factors\ (except\ l, C) \qquad (5)$$

As per ASME BPV Code Case N-871, if a user follows the ASD method to design the CFRP repair system, they are not required to determine various strength reduction factors for their specific application and materials as they will be using the Code Case recommended factor of safety. On the other hand, for LRFD method, the user is required to determine the adjustment factor and time effect factor for their specific material, or provide justification for using Code Case recommended values, but they are not required to determine other strength reduction factors discussed in this report. As some strength reduction factors may have a significant effect (see Eq. 4 and 5) in evaluating the FS_{eff} for any application such as repair of Class 2 and 3 piping using CFRP, it is important to first identify various strength reduction phenomena that may exist over the entire service period of Class 2 and 3 piping, and then determine their effects on the effective factor of safety as discussed in the following section.

1.2 Strength Reduction Phenomena in CFRP Repair System

After reviewing the ASME Code Case N-871, several strength reduction phenomena have been identified by the authors of the report that directly affect the effective factor of safety, FS_{eff} for the specific application of CFRP repair for nuclear Class 2 and Class 3 safety related piping. These strength reduction factors are related to design specifications, installation procedures or criteria and in-service properties degradation as listed below.

i. Variation in statistical analysis of ultimate strength
ii. Effect of multi-ply laminate
iii. Effect of misalignment angle
iv. Time effect factor due to sustained loading
v. Materials adjustment factors due to harsh environmental exposure
vi. Effect of temperature

Each one of the above phenomena has a detrimental effect on the performance of CFRP materials, especially on the strength values such as tensile, flexural and bond strength. Their effects can be quantified through a series of coupon tests as described in subsequent sections. It is pertinent to mention that some of the strength reduction phenomena are related to short-term loading while others are related to long-term. For example, environmental exposure and time effect factors are caused by long-term loading and affect the performance of the CFRP repair systems when they are in-service for a long time (50 years of service) and their effect may vary over the length of service period. Whereas the short-term reduction factors such as effect of temperature affect the performance of the repair system immediately, and do not vary with time. Identifying the short-term and long-term factors would facilitate in evaluating the FS_{eff} for short-term and long-term use. The following sections briefly describe various strength reduction phenomena that may exist in the CFRP repair system when they are in-service for long period (e.g., 50 years).

1.2.1 Variation in statistical analysis of ultimate strength – to experimentally determine the strength reduction factor due to the variation in statistical analysis of ultimate strength

Because composite materials are known to show large variation in mechanical properties, the property values are statistically determined and given as an average value such as "characteristic value" or "basis value" that accounts for this variation and uncertainty. There are three characteristic or basis values that have been used in civil engineering and aerospace industries: the characteristic, A-basis and B-basis values. The characteristic value is defined as a 5^{th} percentile value with 80% confidence, whereas the A-basis and B-basis values are defined as 1^{st} and 10^{th} percentile values with 95% confidence for a particular probability distribution of an appropriate sample size (typically the sample size is 50 or more for evaluating composite properties). In simple terms, the characteristic value (5^{th} percentile) indicates that 95% of sample data (composite property) are at or above the characteristic value whereas A-basis (1^{st} percentile) and B-basis (10^{th} percentile) values indicate that 99% and 90% of sample data are at or above the A-basis and B-basis values respectively. In that regard, A-basis value would be more conservative and B-basis value would be less conservative as compared to the characteristic value from safety and regulatory perspective. The characteristic value is evaluated according to ASTM D7290 [11] which is based on the work of Ellingwood and Zureick [12, 13] specifically developed for civil engineering materials. A-basis and B-basis values are widely used in aerospace industry [14-16]. It is important to note that A-basis strength value, which is most conservative is applied to a single primary component whose failure would cause loss of structural integrity, while the B-basis value is applied to components where the load would be safely redistributed after the specific component's failure.

The ASME BPV Code Case N-871, Section 3131 (c) recommends using the characteristic value of ultimate strength of CFRP to determine the allowable design stress. In light of the above discussion, the A-basis value would be more conversative for nuclear safety related applications as compared to the characteristic value. *The difference in the characteristic and A-basis values would reduce the effective factor of safety and hence, it is important to quantify the difference.* The characteristic and basis values of ultimate strength of CFRP can be statistically determined by conducting tensile tests with 50 or more samples. As the strength value is an input to the design equation, this particular strength reduction phenomena affects the short-term safety margin, i.e., the effect will be realized immediately upon the repaired pipe being placed in-service.

1.2.2 Effect of multi-ply laminate - to experimentally determine the effect of multi-ply laminate on the ultimate strength of CFRP.

In a practical application, multiple layers of CFRP are often necessary to meet the strength requirements and ideally, the characteristic values of ultimate strength of multi-ply laminate should be evaluated for such applications by conducting tensile tests on multi-ply laminate specimens. However, since the required test load to fail a multi-ply specimen increases as the number of layers increase, such tests may become impractical and even unreliable due to large load capacity and large gripping pressure requirements (often causing composite specimens to fail at the grip which invalidates the test result). In order to avoid this, the ASME BPV Code Case N-871, Section 3131 (e) has a provision for using the following equation to evaluate the characteristic value of multi-

ply laminates as a function of the strength of a single-ply laminate where n is the number of layers and σ_1 is the strength of single-ply laminate.

$$\sigma_n = [1 - 0.03(n-1)]\sigma_1 \quad \text{for } n \leq 4 \qquad (6)$$

As per Eq. 6, the strength of multi-ply laminate decreases as the number of layers increase by 3% of the strength of a single-ply laminate for each additional layer, e.g., the strength of 2-ply and 3-ply laminate would be 97% and 94% of the strength of single-ply respectively. This is due to the fact that as the number of layers increases, the more variability is introduced in the composites during fabrication such as such alignment of unidirectional fibers among multiple layers, the load-transfer between plies etc. Accordingly, while the absolute load carrying capacity of multi-ply laminate increases linearly with the number of plies, the strength of the multi-ply laminate, that is the load per unit area of the laminate cross-section, does not increase with number of layers (since the nominal thickness of the laminate increases linearly) and hence, the reduction in strength with multi-ply laminates. After reviewing Ref. [9], it was found that the test data developed in those studies were inadequate to support this equation. Ref. [9] provided test results conducted on Tyfo® SCH-41S-1 composites for 3- and 4-layer laminates and their characteristic values were based on only 10 samples from each type (50 samples are recommended as per ASTM D7290). The test results for single-ply laminate for that material is missing as well in the Ref. [9]. *Therefore, the strength reduction factor for multi-ply laminate shown in Eq. 6 needs to be validated by conducting a series of tensile tests with 1-, 2-, 3- and 4-ply specimens.* Similar to the strength of single-ply, strength reduction factor for multi-ply laminates also will affect the short-term safety margin, i.e., the effect is immediate and does not vary with time.

1.2.3 Effect of misalignment angle - to experimentally determine the effect of misalignment angle on the ultimate strength of CFRP.

Section 4360 (a) of the ASME BPV Code Case N-871 allows an in-plane fiber misalignment not exceeding 1 inch over a 12-inch length during installation, which corresponds to a misalignment angle of about 5°. Unidirectional CFRP provides maximum strength along the fiber direction, i.e., 0° due to their anisotropic behavior and any deviation such as allowable misalignment angle from the fiber direction will result in decrease in strength. *Code Case N-871 currently does not provide any technical basis to estimate the strength reduction due to the allowable ~5° misalignment angle.* The strength reduction factor for misalignment angle can be determined by conducting tensile tests on single-ply CFRP laminates with ~5° off-axis tensile specimens and comparing the results with those without any misalignment (0°). Strength reduction factors for allowable misalignment angle affects the short-term safety margin, i.e., the effect is immediate and does not vary with time.

1.2.4 Time effect factor due to sustained loading - to experimentally determine the effect of sustain loading on the ultimate strength of CFRP.

CFRP material is known to have degradation of properties under sustained loading, this factor is denoted by the symbol λ. This is the time effect factor that accounts for the creep and creep rupture of material under sustained loading for the period of service life. Ref. [9] includes a literature survey based on which the recommended time effect factor is 0.8 for CFRP for 50 years

of service and is based on a creep rupture model from Ref. [17] along with experimental results from Ref. [18, 19, 20, 21]. *The ASME BPV Code Case N-871, Section B-1-220 adopted this recommendation with some additional conservatism and recommends using time effect factors of 0.6 (instead of 0.8 in Ref [9]) for CFRP for 50 years of services.* The time effect factor affects the long-term safety margin, i.e., the strength value decreases with time. Typically, for polymers and polymeric composites linear extrapolation of values up to one decade on the logarithmic time scale is allowed. For example, the time effect factor for 50 years of service is 0.6 but it is 0.8 for 5 years of service as per the ASME BPV Code Case N-871, Section B-1-220 (b).

1.2.5 Materials adjustment factors due to harsh environmental exposure to experimentally determine the effect of harsh environment on the ultimate strength of CFRP.

CFRP material is known to have degradation of mechanical properties including strength during their service life when exposed to harsh environments such as deionized water, salt-water, alkali etc. The rate of property degradation may vary with the type of loading such as tensile, flexural, or lap shear as well as with the exposure temperatures. This degradation is accounted for using the materials adjustment factor, C in the design calculation of CFRP repair system.

Long-term durability tests, i.e., mechanical tests on environmentally exposed specimens (for certain periods) are conducted to determine the material adjustment factors for strength and modulus for different loading types and different environments (e.g., water, salt-water). There are a handful of publications [9, 22-25] that have reported some long-term durability test results for CFRP materials which showed that the material adjustment factor for flexural strength can be as low as 0.45 in water at 140 F for 50 years of service life.

Based on the above literature, the effect of the variables on the material adjustment factors are summarized as follows:

- Temperature – Material adjustment factors decrease with increase in temperature.
- Exposure environment – Alkali and salt-water show the most degrading effect, whereas deionized water shows moderate degrading effect.
- Exposure Time – Material adjustment factors decrease with increase in exposure time.
- Number of plies – Material adjustment factors decrease with an increase in number of layers.
- Loading conditions – Material adjustment factors vary with loading conditions.
    - Material adjustment factor for strength is the lowest under flexural loading.
    - Material adjustment factor for modulus is the lowest under lap shear loading.
    - Material adjustment factor for strength is moderate under tensile loading.

The ASME BPV Code Case N-871, Section B-1-200 provides guidance on the above material adjustment factors based on the references above [3, 22-25]. *However, the reported material adjustment factors do not capture the worst-case scenario. For example, the worst-case condition for the current application of CFRP repair on nuclear Class 2 and Class 3 safety related piping would be exposure of multi-ply CFRP laminates to salt-water or alkali solutions at the maximum operating or accident temperatures for the duration of expected service life. Code Case N-871 only reports material adjustment factors for salt-water at room temperature (72F).* It is therefore important to evaluate the material adjustment factors for the worst-case condition which would eventually affect the long-term safety margin of the CFRP repair system.

1.2.6 Effect of temperature to experimentally determine the effect of temperature on the ultimate strength of CFRP.

It is well known that the glass transition temperature, T_g of any thermoset polymer such as epoxy may have a significant effect on mechanical properties at various temperatures. The effect of elevated temperature on CFRP properties is currently being investigated in a separate NRC project at Emc^2 (Project No. RES-19-0237). *Some limited test results indicated that the mechanical properties of CFRP materials can be adversely affected by elevated temperature and can have a significant effect if the curing temperature and resulting T_g of the composite is lower than the test temperature (which is equivalent to design temperature) by a certain amount.* This work is still ongoing, and the results will be reported once they are available. Once evaluated, the effect of temperature on the mechanical properties of CFRP needs to be included in evaluating the effective factor of safety of CFRP repair system.

1.3 Recent Update on Code Case N-871

The preliminary results from the current work were presented by Emc^2 at an NRC Public Meeting "Composite Repair Technical Information Exchange" on January 16, 2020 [26]. Based on the discussion at the meeting, the ASME Task Group (TG) repair by CFRP decided to revise the ASD method in the design section (Section 3000) of Code Case N-871-1. In the revised version, the TG members plan to include the time effect factor, materials adjustment factor, and the effect of temperature in the ASD method. However, there are other strength reduction factors (as discussed in this report) that should be included in the ASD method as well. This revised Section 3000 of Code Case N-871-1 is still under review by the TG members.

2. OBJECTIVES AND APPROACH

The overall objective of the current work is to evaluate and confirm the available margins in Class 2 and 3 degraded piping repaired by CFRP as per ASME BPV Code Case N-871. The following confirmatory experiments were conducted to achieve the overall objective:

- Various confirmatory coupon testing to evaluate various strength reduction factors and minimum bond strength requirements,
- Confirmatory small-scale hydrostatic watertightness tests to determine leakage pressure, and,
- One confirmatory full-scale hydrostatic test of a degraded pipe with CFRP repair under short-term loading condition

At first, various coupon tests were conducted to evaluate the mechanical properties of CFRP as well as determining the various strength reduction factors. These values are the input parameters for the design calculations of CFRP repair system as per the ASME BPV Code Case N-871. Next, the design calculations were conducted for short-term loading conditions (i.e., design pressure and room temperature) to determine the required number of composite layers in CFRP repair system as per Code Case N-871. The small-scale watertightness test was then conducted using the as-designed CFRP repair system to ensure the watertightness of the system as per the ASME BPV Code Case N-871. Finally, a 40-inch diameter degraded steel pipe with a 12-inch x 24-inch hole was repaired with CFRP as per ASME BPV Code Case N-871 and a full-scale hydrostatic test of the repaired pipe was conducted at room temperature (72 F) with stepwise increases of pressure

until failure occurred. The available margin was calculated for short-term loading using failure and design pressures. Various instrumentations such strain gages, thermocouples, pressure transducers were installed during the full-scale hydrostatic test to monitor the several variables during this test and to provide additional insight on CFRP installation and failure process.

3. DETERMINATION OF VARIOUS STRENGTH REDUCTION FACTORS

The following section describes various coupon tests conducted to determine several strength reduction factors discussed in Section 1.2 such as variation in statistical analysis of ultimate strength, effect of multi-ply laminate, effect of misalignment angle. Note that determination of the other strength reduction factors such as materials adjustment factors due to harsh environmental exposure, time effect factor due to sustained loading and effect of temperature was outside the scope of this effort and is currently being investigated in a separate NRC project (except time effect factor). An update on the ongoing investigation of remaining strength reduction factors is also given towards the end of this section.

3.1 Variation in Statistical Analysis of Ultimate Strength

At least 50 tensile tests are required to perform the statistical analyses to determine the characteristic (as per Code Case N-871 using ASTM D7290), A-basis and B-basis values of ultimate strength of single-ply CFRP laminate. For this effort, unidirectional CFRP panels and tensile specimens were procured from Structural Technologies Inc., a CFRP material supplier[*]. The CFRP panel was fabricated using V-Wrap™ C400HM unidirectional carbon fiber (0.08-in nominal thickness) and V-Wrap™ 770 epoxy. Material safety data sheets (MSDS) along with technical data for this CFRP pane are given in Appendix A. More than 50 tensile tests were conducted according to ASTM D3039 at room temperature in two laboratories. Emc^2 subcontracted Simpson, Gumpertz & Heger (SGH), Inc. to conduct 50 tensile tests while at least five additional confirmatory tests were also conducted in the Emc^2 laboratory. Figure 1 shows the stress-strain curves for all tensile tests from both laboratories and the ultimate strengths for all specimens are shown in Figure 2. As seen in these two figures the test results from both laboratories are consistent and repeatable and the percent differences in average ultimate strength and modulus between the two laboratories are within 2-3%. The details for all tensile tests are provided in Appendix B. The average values of ultimate strength and modulus with their co-efficient of variance (COV) are given in Table 1. Note that the effect of curing temperature and time, glass transition temperature and design temperature on the mechanical properties of CFRP materials has not been investigated; however, some of these are being investigate in another related NRC program which is still ongoing.

[*] Structural Technologies installed the CFRP repair at the Surry Nuclear Power Station per their Relief Request approved by the NRC.

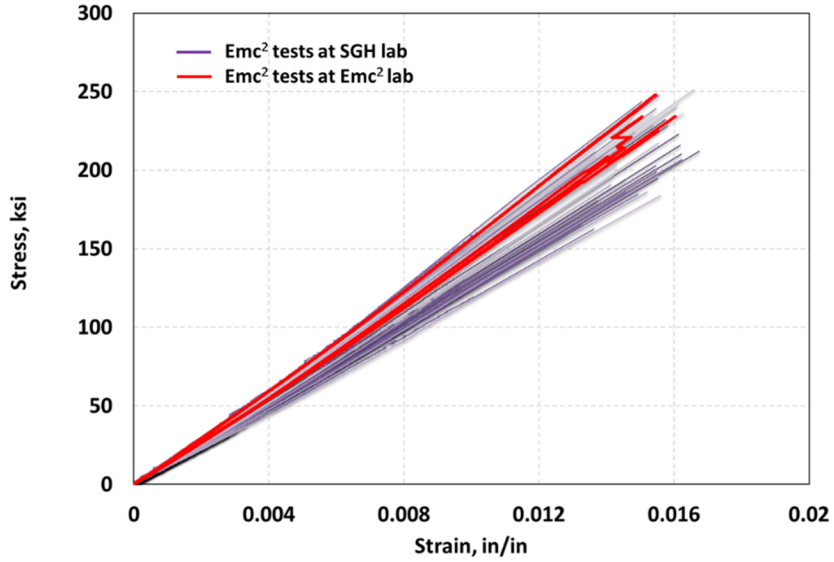

Figure 1 Tensile test results for single-ply CFRP laminate

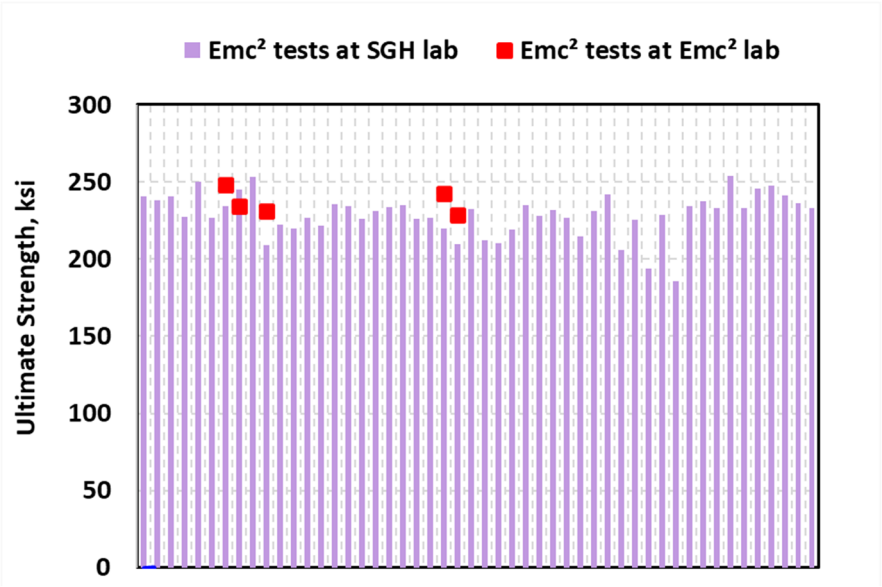

Figure 2 Ultimate strength of single-ply CFRP laminate

Table 1 Tensile test results for single-ply laminate

Tensile Properties	Average	COV
Ultimate Strength, ksi	229.7	5.9%
Modulus, msi	14.056	4.7%

Statistical analyses of all tensile test results, i.e., ultimate strengths of single-ply laminates were performed to determine the characteristic, A-basis, and B-basis values. The distribution curves are shown in Figure 3 and the values are reported in Table 2. As seen in Table 2, the ASME BPV Code Case N-871 recommended ASTM D7290 characteristic value (5th percentile with 8-% confidence) is 11% higher than the A-basis (1st percentile) value and only 2% lower than the B-basis (10th percentile) value. *In other words, A-basis value provides more conservative (by 11%) ultimate strength value of CFRP as compared to Code Case recommended characteristic value. For nuclear safety-related applications, it is therefore recommended to either use A-basis values of ultimate strength or use a strength reduction factor of 0.89 (i.e., 1.00-0.11) on the characteristic values for C400H*. While we anticipate that this factor might have some level of variability for different materials, the results provide a quantitative estimate of the strength reduction factor for variation in statistical analysis based on actual experiments on CFRP materials recommended for use in nuclear safety-related applications.

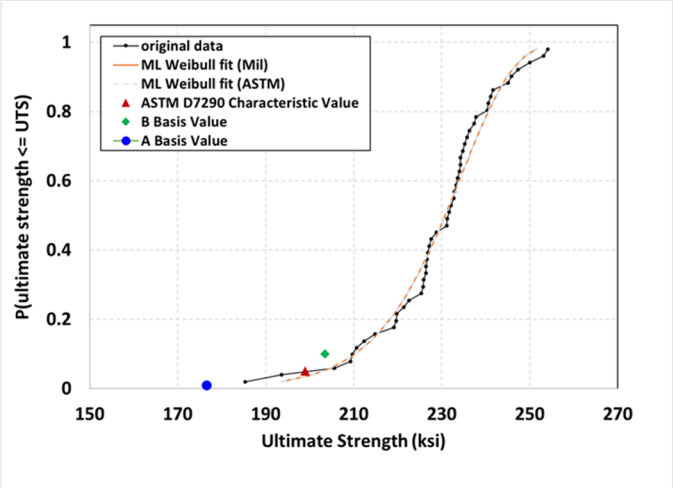

Figure 3 Statistical analyses of single-ply CFRP (C400H) laminate tensile tests

Table 2 Characteristic values of ultimate tensile strength for single-ply CFRP (C400H) laminate

Methods	Characteristic Values of Ultimate Strength, ksi	Difference with CC-N871
ASTM D7290 (CC N-871)	198.9	-
A Basis	176.5	-11%
B Basis	203.5	2%

3.2 Strength determination for Multi-Ply Laminates

As explained above, while the absolute load carrying capacity (lbs) of the multi-play laminates increases with the number of plies, the strength (psi) of the multi-ply laminates decreases. This reduction in strength of multi-ply laminates is given in the form of Eq. 6 (repeated below for convenience). Data from at least 50 tensile tests for each of 1, 2, 3 and 4 ply specimens

are required to calculate the characteristic values of ultimate strength of each specimen type. Note that CC N-871 suggests using Eq. 6 below to determine the strength reduction factors for 1, 2, 3 and 4 ply laminates. The goal is to experimentally verify if Eq. 6 provides a conservative estimate of ultimate strength of multi-ply laminates. Additionally, these test results can also be used to perform various statistical analyses to evaluate the variation in ultimate strength (similar to Section 3.1) for multi-ply laminates.

$$\sigma_n = [1 - 0.03(n-1)]\sigma_1 \text{ for } n \leq 4 \qquad (6)$$

where n is number of plies, σ_1 and σ_n are the characteristic values of ultimate strength of 1 and n plies, respectively.

The 1, 2, 3 and 4 ply tensile specimens have been prepared using V-Wrap™ C200H unidirectional carbon fiber (0.04 in nominal thickness) and V-Wrap™ 770 epoxy from Structural Technologies Inc. Note that the carbon fiber used for multi-ply laminate tests (V-Wrap™ C200H) is lighter and thinner than that used in the single-ply laminate tests in Section 3.1 (V-Wrap™ C400H). This is due to the fact that load carrying capacity of C400HM is so high that it is very difficult to perform a valid tensile test using ASTM D3039. Most or all multi-ply specimens (C400H) tend to fail at the grip. It is relevant to mention that thicker carbon fiber (C400H) is used in the repair of the repairing safety related piping at Surry Power Station in 2016, per the relief request that was approved by the NRC. Nevertheless, it was possible to have valid tensile tests for all four specimen types, i.e., 1-ply, 2-ply, 3-ply and 4-ply using the C200H carbon fiber (thinner fiber) which is adequate to verify Eq. 6.

Emc^2 subcontracted with SGH to conduct at least 50 tensile tests for each specimen type. A few additional confirmatory tests for each specimen type were also conducted in the Emc^2 laboratory to verify the range of SGH test data. Because of the small sample size, statistical analyses were not conducted on Emc^2 test data. To keep the discussion in this section focused on the overall objective, i.e., strength reduction in multi-ply laminates (compared to single-ply laminate), only those tests conducted at SGH have been statistically analyzed and compared. However, the details of all tensile test results for multi-ply laminates conducted at both SGH and Emc^2 laboratories are given in Appendix C.

Figure 4 shows the ultimate strengths of 1-ply, 2-ply, 3-ply and 4-ply specimens tested at SGH laboratory. Statistical analyses of the ultimate tensile strengths were performed to determine the characteristic values according to ASTM D7290 for each of the four specimen types, i.e., 1-ply, 2-ply, 3-ply and 4-ply laminates. The curves showing the distribution of the strength values are illustrated in Figure 5. Both A-basis and B-basis values of the four specimen types were also determined according to MIL Handbook 17 [14, 15]. As per Eq. 6, only characteristic values for each specimen type are used to verify Eq. 6 whereas A-basis and B-basis values are used to evaluate the variation in statistical method for multi-ply laminates.

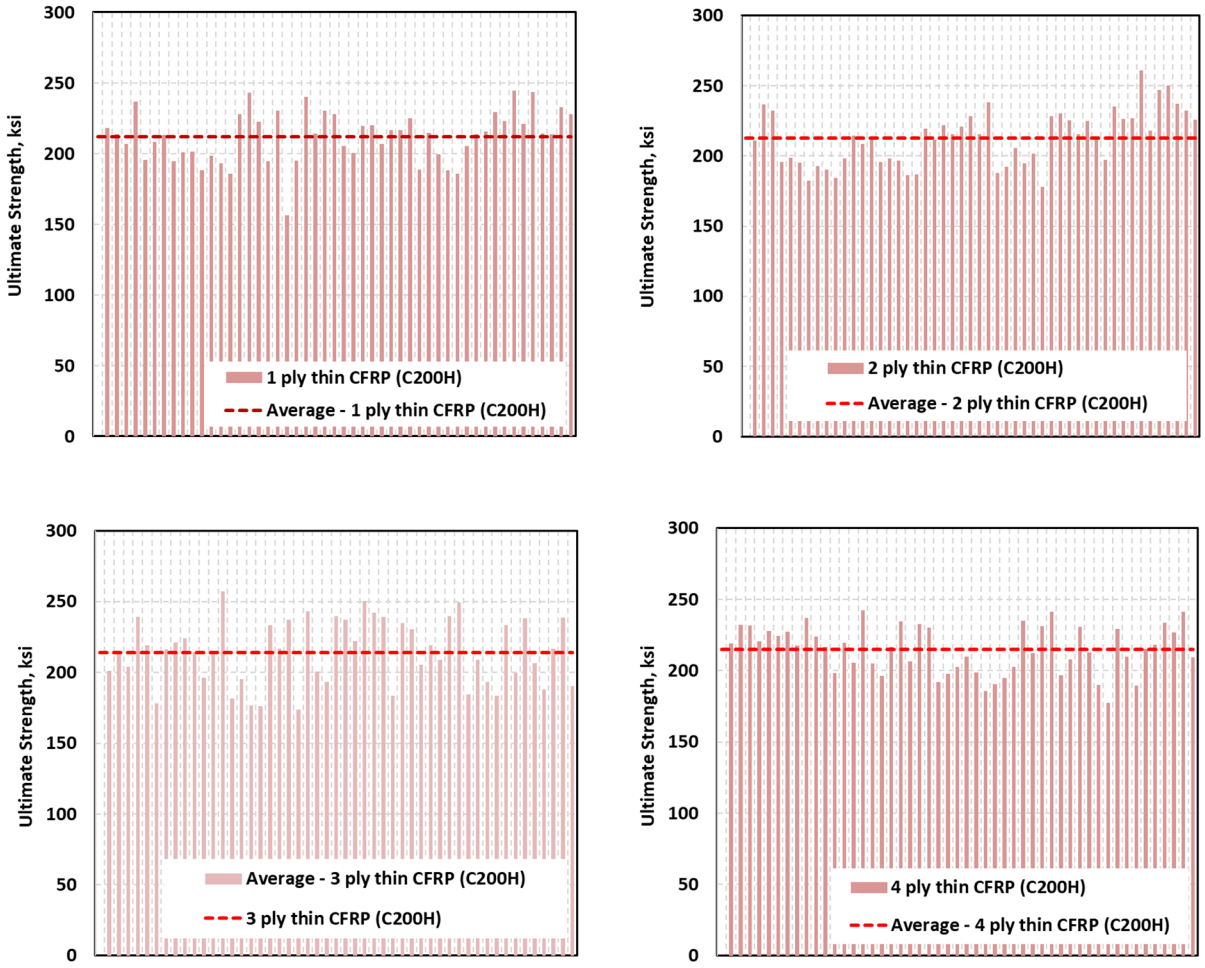

Figure 4 Ultimate strength of single and multi-ply CFRP (C200H) laminates tested at SGH and Emc²

All calculated statistical tensile strength values are reported in Table 3 which also includes the strength reductions for multi-ply laminates as compared to the strength of the single-ply laminate. As seen in Table 3, the characteristic values of the ultimate strength for 2-ply, and 3-ply laminates are 3.8% and 4.6% lower than their corresponding single-ply results respectively. Interestingly, the 4-ply tensile specimens showed higher characteristic values of strength than that for single-ply specimen (about 3.7% higher). As per Eq. 6, the ASME BPV Code Case N-871 recommended reduction factors for 2-, 3- and 4-ply laminates are 3%, 6% and 9% lower than the single-ply values. *Based on these experimental data, Eq 6 seems to be conservative for 2-ply and 3-ply laminates and slightly non-conservative for 4-ply laminate.*

This test data was also used to determine the percent difference in strengths using statistical analysis method (similar to Section 3.1) as reported in Table 4. As seen in the table, the characteristic values of ultimate strengths are 15-20% higher (non-conservative) than the A-basis values and only 3-4% lower than B-basis for single- and multi-ply CFRP (C200H) laminates. Note that the strength reduction factors are only applied to the strength of single-ply laminate. In this

regard, the difference between characteristic and A-basis values for single-ply C200H CFRP laminate is 16%. *Therefore, the strength reduction factor due to the statistical variation for single-ply laminate would be 0.84 for C200H (as compared to 0.89 for C400H).*

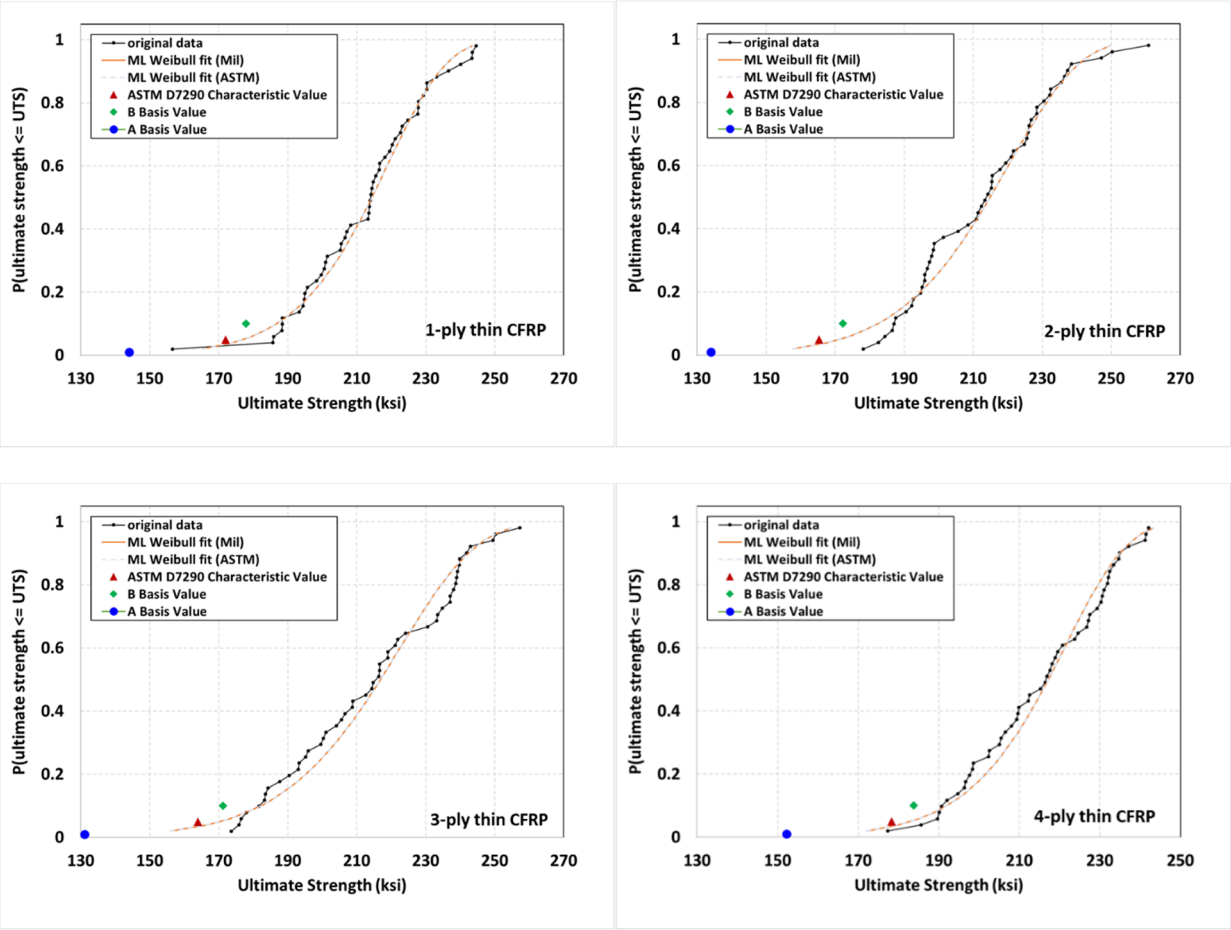

Figure 5 Determination of characteristic and basis values of ultimate tensile strengths for 1-ply, 2-ply, 3-ply and 4-ply CFRP (C200H) laminate

Table 3 Characteristic and basis values of ultimate tensile strengths for 1-ply, 2-ply, 3-ply and 4-ply CFRP (C200H) laminate showing strength reduction for multi-ply laminate

Statistical Methods	1-Ply	2-Ply	3-Ply	4-Ply	Difference with 1-ply		
					2-Ply	3-Ply	4-Ply
Characteristic values	172.0	165.4	164.0	178.3	-3.8%	-4.6%	3.7%
A Basis	144.1	134.0	131.1	152.2	-	-	-
B Basis	177.9	172.2	171.3	183.8	-	-	-
Code Case recommended multi-ply reduction factor (Eq. 5)					-3%	-6%	-9%

Table 4 Statistical values of ultimate tensile strengths for 1-ply, 2-ply, 3-ply and 4-ply CFRP (C200H) laminate showing variations in statistical analyses

Statistical Methods	1-Ply	2-Ply	3-Ply	4-Ply	Difference with characteristic values			
					1-Ply	2-Ply	3-Ply	4-Ply
Characteristic values	172.0	165.4	164.0	178.3	-	-	-	-
A Basis	144.1	134.0	131.1	152.2	-16%	-19%	-20%	-15%
B Basis	177.9	172.2	171.3	183.8	3%	4%	4%	3%

3.3 Effect of Misalignment Angle

Section 4360 (a) of the ASME BPV Code Case N-871 allows an in-plane fiber misalignment not exceeding 1 inch over a 12-inch length during installation, which corresponds to a misalignment angle of ~5°. Unidirectional CFRP provides maximum strength along the fiber direction, i.e., 0° due to their anisotropic behavior and any deviation such as allowable misalignment angle from the fiber direction will result in a decrease in strength. The strength reduction factor for misalignment angle was determined by conducting tensile tests on single-ply CFRP laminate with ~5° off-axis tensile specimens and comparing the results with unidirectional (0°) tensile results.

The off-axis tensile specimens were prepared such that the loading direction was at $\theta \approx 5°$ angle compared to the fiber direction, as shown in Figure 6. The CFRP panel was fabricated using V-Wrap™ C400HM unidirectional carbon fiber and V-Wrap™ 770 from Structural Technologies Inc (See Appendix A for MSDS and the Technical Data Sheets). As seen in Figure 6, only the yellow-shaded fibers are continuous from grip-to-grip and the width of these continuous fibers in the off-axis tensile specimens is denoted as equivalent width, W′. The equivalent width can be calculated from the full width, W using the equation shown in Figure 6 where L is the gage length and θ is misalignment angle. As the fibers are continuous in the actual pipe repair, the equivalent width should be used to calculate the ultimate strength of the off-axis tensile specimens, and exclude unnecessary conservatism if the full width is used. Two types of 5° off-axis tensile specimens were prepared with two different widths to study the effect of width on the strength of off-axis tensile specimen. The full widths of two specimen types were 1.2 and 1.6 inches and their corresponding equivalent widths are about 0.86 and 1.27 inches. The width of the 0° unidirectional specimen was about 0.9 inch which is very similar to equivalent width of 0.86 inch for one of the off-axis tensile specimens.

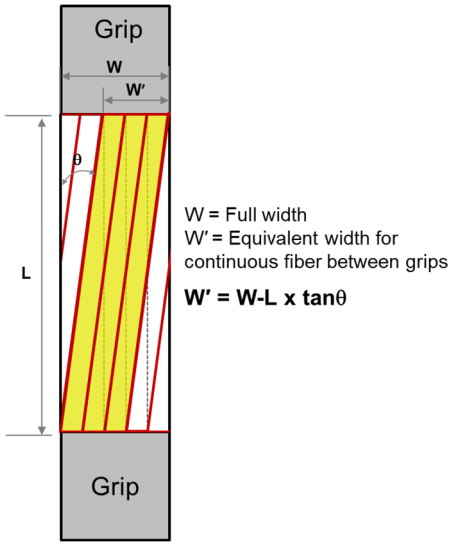

Figure 6 Schematic of off-axis CFRP tensile specimen

A total of 16 off-axis tensile specimens (8 specimens from each type) were tested at the Emc^2 laboratory. Table 5 shows the comparison of the single-ply off-axis test results with those from the unidirectional CFRP laminate.

Figure 7 shows the average values of ultimate strength and modulus of single-ply off-axis and unidirectional CFRP laminates. The details of all tests are provided in Appendix B. As seen in these figures, the average ultimate strengths of the two off-axis specimen types are 20-27% lower than that for unidirectional tensile specimens, whereas the modulus for both unidirectional and off-axis specimens remains the same. As mentioned above, the average equivalent width of the first off-axis specimen type (~0.86 inch) is very close to the average width of the unidirectional specimen (0.9 inch) which showed 27% drop in ultimate strength due to a fiber misalignment angle of 4.7°. However, as the width of the off-axis specimens increased to 1.27 inch, the average strength of the wider off-axis specimens showed about 20% drop in ultimate strength as compared to the strength of unidirectional specimens. *In summary, the strength reduction factor for the allowable misalignment angle (of about 5°) was found to be between 0.73 and 0.80.* A similar effect is also reported in [27] where unidirectional CFRP laminate showed about 14% reduction in strength for 5° misalignment angle.

Table 5 Comparison of single-ply off-axis tensile test results with unidirectional CFRP laminate

Properties	Unidirectional, W≈0.9"		Off-Axis, W′≈0.86"			Off-Axis, W′≈1.27"		
	Average	COV	Average	COV	% Diff. Off-axis/Uni.	Average	COV	% Diff. Off-axis/Uni.
Ultimate Strength, ksi	236.8	3.5%	171.9	7.6%	-27.4%	190.2	6.9%	-19.7%
Modulus, msi	13.93	4.6%	14.23	7.7%	2.2%	14.75	13.3%	5.9%

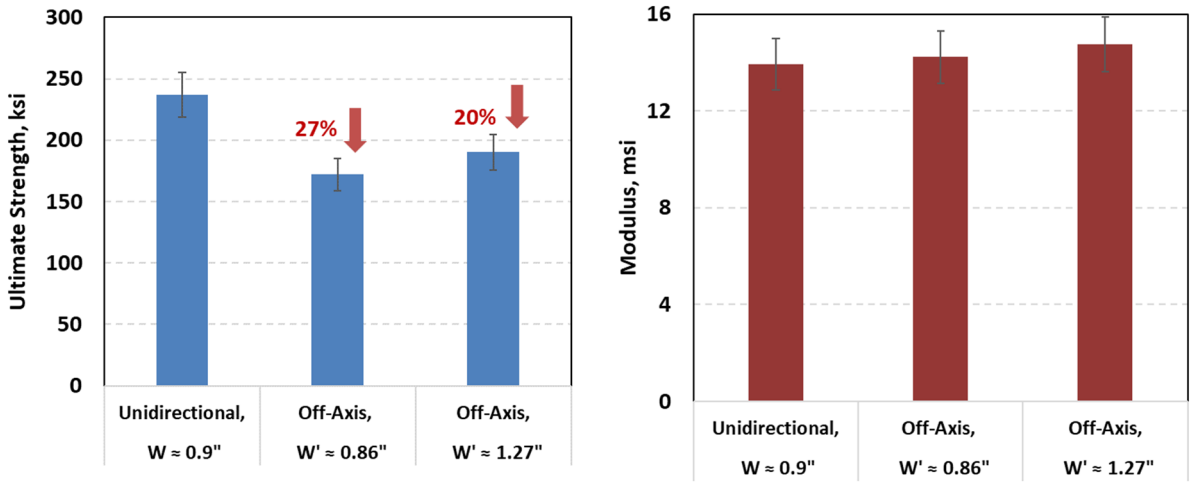

Figure 7 Comparison of ultimate strength and modulus of single-ply off-axis and unidirectional CFRP laminates

3.4 Ongoing Investigation of Remaining Strength Reduction Factors

3.4.1 Long-Term Material Degradation Factors

CFRP materials are known to have degradation of mechanical properties over their service life when exposed to harsh environments such as deionized water, salt-water, alkali etc. This is accounted for with materials adjustment factors, C, in the design calculation of CFRP repairs. The rate of property degradation may vary with the type of loading such as tensile, flexural, or lap shear and shows increase degradation rates at elevated exposure temperatures. ASME BPV Code Case N-871 provides a list of materials adjustment factors for ultimate strength and modulus for environmental exposure (water, salt-water, and alkali) in Table B-1-210-1. *However, Table B-1-210-1 does not capture the worst-case scenario which would be the exposure of multi-ply CFRP laminates to salt-water or alkali solutions at the maximum operating or accident temperatures for the duration of expected service life. This is being addressed in a separate NRC project at Emc^2 (Project No. RES-19-0237) where specimens are being prepared and exposed to salt-water solution at 140 F for long-term durability tests and various mechanical tests will be conducted in the future as specimens become available after exposure. These test results will be analyzed to determine the worst-case (salt-water at elevated temperature) materials adjustment factors.*

In this report, the worst-case condition of materials adjustment factors reported in Table B-1-210-1 is used as an example case to evaluate the impact on the effective factor of safety in a later section. However, the calculations should be updated if ongoing efforts reveal that the materials adjustment factors (for salt-water at elevated temperature) are lower than the corresponding values reported in Table B-1-210-1. Nevertheless, as per Table B-1-210-1 in ASME BPV Code Case N-871, the worst-case material adjustment factors for environmental exposure for 50 years of service are 0.45 and 0.55 for flexural strength and lap shear strength in water at 140 F respectively.

3.4.2 Effect of Temperatures

There are three temperatures namely curing temperature (T_c), glass transition temperature (T_g) and test or design temperature (T_{op}) that influence the physical, thermal and mechanical properties of polymer materials. The glass transition temperature, Tg is the temperature below which the physical properties of plastics change in a manner similar to those of a glassy or crystalline state, and above which they behave more as a rubbery material [28]. The cure temperature is the temperature at which the polymer is cured that affects the crosslinking of polymeric chain and hence, influences the T_g. The test or design temperature is the temperature at which the polymeric materials are tested or the temperature under service conditions.

Previous studies for several epoxy materials in literature have shown that Tg increase with the increase of T_c until a certain temperature above† which T_g may drop or reach plateau [29-34]. Since T_g is the measure of crosslinking density (i.e., molecular mobility), mechanical properties of the polymer at a particular test temperature increase with the increase of T_g until reaching a plateau or dropping [29-34]. Note that above tests are conducted at room temperature (well below T_g for all cases). However, this literature survey provides some understanding about the correlation between T_c and T_g and their effect on mechanical properties.

The effect of test temperature (i.e., design temperature) on CFRP properties is being investigated in a separate NRC project at Emc^2 (Project No. RES-19-0237). Some limited test results indicate that the mechanical properties such as tensile, lap-shear, pull-off and flexural strengths of CFRP materials can be adversely affected by elevated test temperature. Preliminary coupon test results from this related effort confirm that the mechanical properties of CFRP materials are significantly reduced when the test temperature is higher than the curing temperature by a certain amount (55F). This work is still ongoing and focuses on how much the strengths of CFRP materials degrade at elevated temperature and what should be the allowable temperature difference (between maximum design temperature and T_g). Once completed, the strength reduction factor of temperature effect should also be included in the design equation to evaluate the margin in the effective factor of safety.

Another important point to note is that the effect of temperature can be coupled with materials adjustment factors which depends on how the durability tests are conducted to determine the materials adjustment factors. After exposing the specimens to harsh environment at elevated temperature for certain time, if durability tests are conducted at elevated temperature, then the effect of temperature is included in the materials adjustment factors and therefore do not need to evaluate separately. If the test is conducted at room temperature (even if the exposure is at an elevated temperature), then the effect of temperature needs to be included separately.

3.5 Summary of Various Strength Reduction Factors

This section provides the summary of various strength reduction factors that will be used in evaluating the effective factor of safety, FS_{eff} of the CFRP repair system. Table 6 shows the list of all strength reduction factors where strength reduction factors due to variations by statistical methods, effect of multi-ply laminates and misalignment angle are determined experimentally in the current program. ASME BPV Code Case N-871 recommends this value be used for time effect factor due to sustained loading. As efforts in a separate NRC program for experimentally

†This temperature is called $T_{g\infty}$ defined as the glass transition temperature of ***fully*** cured polymers.

determining the material adjustment factors (environmental effect) are ongoing, the worst-case values for the material adjustment factor reported in Table B-1-210-1 in ASME BPV Code Case N-871 are used in Table 6. In the same NRC program, the effect of temperature is also being investigated.

Table 6 List of various strength reduction phenomena for CFRP repair system

Various strength reduction phenomena	Strength reduction factors	Comments
Variation in statistical analysis, C_s	C_s = 0.84-0.89	Values are experimentally determined in the current project
Strength reduction in multi-ply laminates	0.97 for 2-ply 0.94 for 3-ply 0.91 for 4-ply	Values are determined using CC N-871, Section 3131 (e) which is also verified experimentally in the current project
Effect of misalignment angle, C_θ	C_θ = 0.73-0.8	Values are experimentally determined in the current project
Time effect factor due to sustained loading, λ	50 years, λ=0.6 5 years, λ=0.8	Values are taken from CC N-871, Section B-1-220 (b)
Materials adjustment factors due to harsh environmental exposure, C	C= 0.45 for flexure C = 0.55 for lap shear	Lowest values* are taken from CC N-871, Table B-1-210-1
Effect of temperature, C_T	Tests are ongoing to evaluate the effect of temperature in another NRC project	

** CC N-871, Table B-1-210-1 does not capture the worst-case condition and a separate NRC program is currently ongoing to evaluate the materials adjustment factors under worst condition.*

4. BOND STRENGTHS AT TERMINAL ENDS

Terminal ends are defined as the portion of CFRP repair at each end of a degraded segment and are structurally bonded to the pristine steel substrate. To prevent CFRP laminate from debonding from the steel substrate at CFRP terminations, the CFRP repair system must provide sufficient bond strength to accommodate design loadings at the terminal ends. Normally, lap shear and pull-off tests are used to determine these bond strength properties. As per ASME Code Case N-871, Section 3131.1, the minimum pull-off strength and shear strength of CFRP to steel substrate is recommended to be 700 psi and 1100 psi, respectively. However, these minimum values are recommended based on previous experience per the ASME Task Group's response to an Emc^2/NRC comment on the Code Case. In order to ensure that the CFRP repair system has sufficient bond strength to successfully perform a full-scale hydrostatic test with CFRP repair in the current workscope, coupon tests were conducted to determine the bond strength of the CFRP repair system. Also, it is noted that CFRP repair systems are installed over an initial dielectric Glass Fiber Reinforced Polymer (GFRP) layer which is in contact with the host degraded metallic pipe. The host pipe in any specific application could be made of different metallic materials such as steel or aluminum-bronze alloys and it is well-known that bond and lap shear strengths of

adhesives can be significantly affected by the substrate material. Therefore, it is important to evaluate the bond and lap shear strengths of GFRP laminates on various metallic substrates.

4.1 Lap Shear Strength

Since the GFRP layer (dielectric layer) of the CFRP repair system is the first layer that adheres to the host pipe, two types of lap shear specimens were prepared using V-Wrap EG50-B bi-directional (±45°) glass fiber (see MSDS and Technical Data Sheets in Appendix A for details) and V-Wrap™ 770 epoxy from Structural Technologies Inc. on two metallic substrates – steel and aluminum-bronze alloys. For steel substrates, two types of specimens were prepared according to ASTM D5868 for single lap shear and ASTM D3528 for double lap shear. Note that double lap shear tests are often recommended to be used to evaluate the lap shear strength as single lap shear specimens tend to cause out-of-plane bending during the test due to the eccentricity of the single lap shear specimen design which typically provides lower shear strength. Even though the composites in the actual pipe repair would be similar to a single-lap joint, it would not have any eccentric loading. Nevertheless, both single lap joint and double lap joint specimens were prepared with steel substrates to investigate the effect of the two specimen designs on lap shear strengths. However, only double lap shear specimens were prepared for aluminum-bronze alloy substrates as it avoids eccentricity of loading.

Table 7 shows the lap shear results for both steel and aluminum-bronze substrates. Figure 8 shows single and double lap shear results for GFRP on steel substrates and Figure 9 shows the comparison of double lap shear results for GFRP on steel and aluminum-bronze substrates. As seen in the table and Figure 8, double lap shear specimens showed higher average shear strength by about 24% as compared to single lap shear specimens, as expected.

The most relevant test data for the current design of CFRP repair are shown in Figure 9 – the comparison of double lap shear results for GFRP on steel and aluminum-bronze substrates. As seen in this figure, the average shear strengths for GFRP are 2,044 psi and 1,537 psi and the minimum shear strength values are 1,604 psi and 1,220 psi, for steel and aluminum-bronze substrates, respectively. Therefore, the shear performance of GFRP on a steel substrate is better than on an aluminum-bronze alloy substrate. However, both substrates showed minimum shear strengths that are higher than the minimum recommended shear strength of 1,100 psi in Code Case N-871.

Table 7 Lap shear results for GFRP on steel and aluminum-bronze substrates

Test Method	Fiber Material	Substrate Material	Minimum Shear Strength, psi	Average Shear Strength, psi	COV
Double lap shear	GFRP	Steel	1604	2044	10.4%
Single lap shear	GFRP	Steel	1347	1546	7.5%
Double lap shear	GFRP	Aluminum-bronze	1220	1537	18.0%

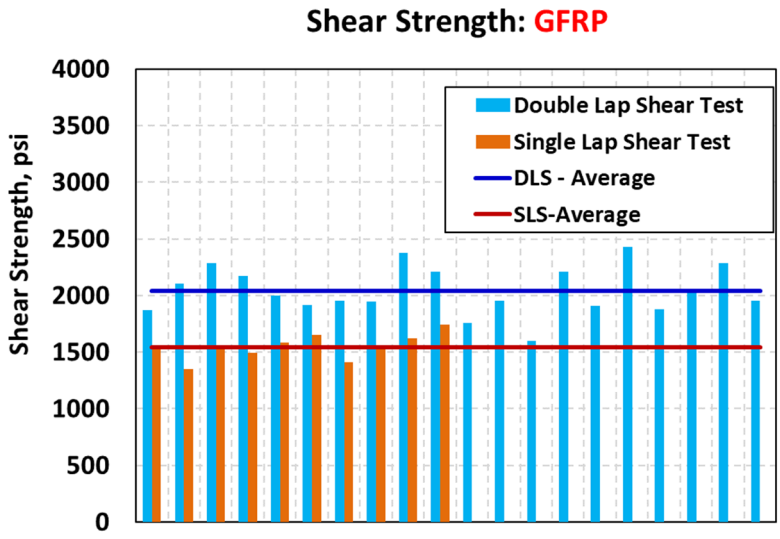

Figure 8 Single and double lap shear test results for GFRP on steel substrates

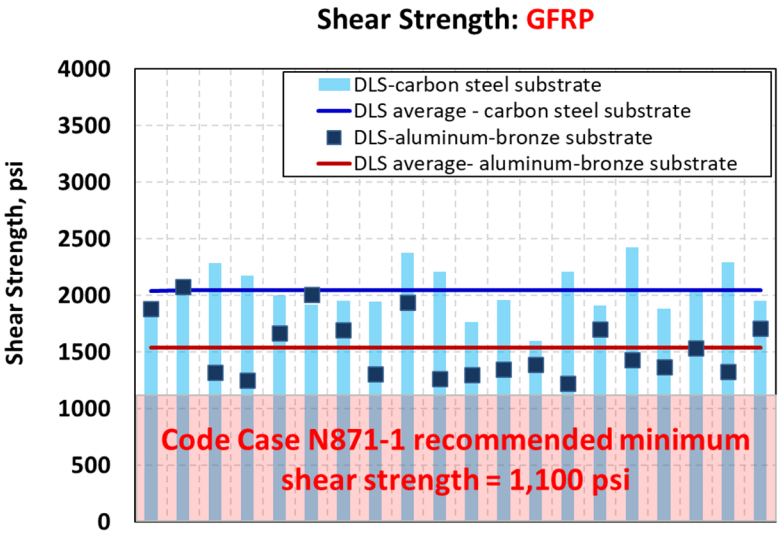

Figure 9 Double lap shear test results for GFRP on steel and aluminum-bronze substrates

4.2 Pull-off Strength

Two types of pull-off specimens were prepared using V-Wrap EG50-B bi-directional (±45°) glass fiber and V-Wrap™ 770 epoxy (see MSDS and Technical Data Sheets for details in Appendix A) from Structural Technologies Inc. on two metallic substrates – steel and aluminum-bronze alloy – according to ASTM D4541.

Table 8 and Figure 10 show pull-off test results for GFRP on steel and aluminum-bronze substrates. As seen in the table and figure, average and minimum shear strengths are much higher for aluminum-bronze substrate than the steel substrate – an opposite trend as compared to shear strengths on these two substrates. For aluminum-bronze substrate, the average (2,864 psi) and minimum (2,257 psi) pull-off strengths are significantly higher than the minimum pull-off strength requirement of 700 psi. However, for steel substrate, one out of ten specimens showed pull-off strength of 424 psi which is less than the minimum requirement while the other nine specimens showed pull-off strengths higher than 700 psi with an average strength of 1,263 psi. Post-test failure analysis of the low value steel substrate test did not provide any specific indication of lower pull-off strength of that specific test. Moreover, coefficient of variance for the steel substrate was also much higher (33%) as compared to aluminum-bronze substrate (11%).

Table 8 Pull-off test results for GFRP on steel and aluminum-bronze substrates

Fiber Material	Substrate Material	Minimum Pull-off Strength, psi	Average Pull-off Strength, psi	COV
GFRP	Steel	424	1263	33%
GFRP	Aluminum-bronze	2257	2864	11%

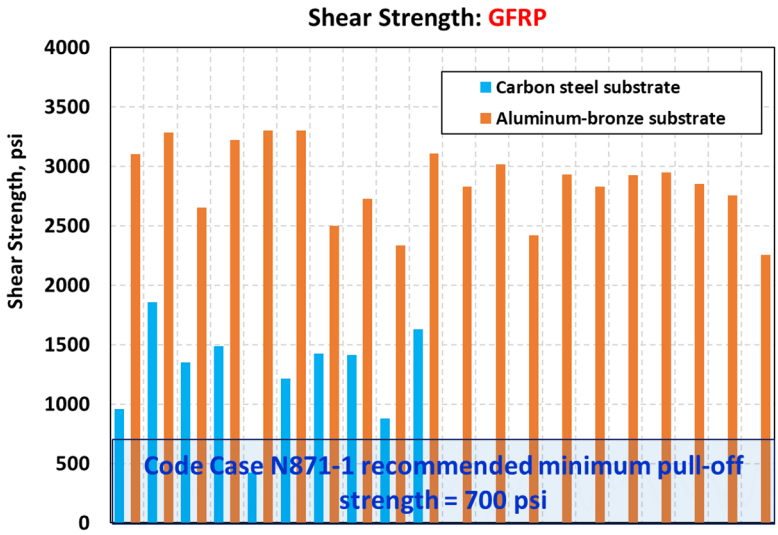

Figure 10 Pull-off test results for GFRP on steel and aluminum-bronze substrates

5. EFFECTIVE FACTOR OF SAFETY, FS_{eff} FOR CFRP REPAIR SYSTEM

Since CFRP materials are relatively new in safety-related nuclear applications, the ASME BPV Code such as Sections II, III or VII currently do not have a factor of safety (FS) recommendation for a CFRP material. In order to decide on a reasonable factor of safety for CFRP

materials for nuclear safety related piping applications, ASME BPV Code (for nuclear safety related piping application perspective) and MIL-Handbooks [12-14] from aerospace industry (for composite materials perspective) have been reviewed. As per ASME BPV Code, the factor of safety for cast iron (brittle material) is equivalent to 10, given as $S_u/10$ in Section VIII, Division 1, non-mandatory Appendix P, Table P-1 [35], with S_u being the ultimate strength of the material. Alternatively, the factor of safety for ductile steel is 3.5 on minimum ultimate strength according to ASME BPV Code Section II Part D, Mandatory Appendix 1, Table 1-100. On the other hand, a factor of safety of 1.5 is used on ultimate strength for composite materials as described in Mil-Handbooks for various safety applications in aerospace industry. In the aerospace industry, the manufacturing processes are conducted in a controlled environment inside autoclaves whereas the hand lay-up is used in-situ in the current application of CFPR repair of in-service degraded pipe. Moreover, the degradation of properties (strength reduction factors) of composite materials has been accounted for in performance evaluations as per MIL-Handbook. In aerospace design, materials go through a robust performance evaluation and testing program and it can take over a decade before a new material is added to the approved material database for design [36]. Based on the above discussion on FS from both perspectives – nuclear safety related applications and composite materials, an *effective* factor of safety of 3.5 is deemed to be adequate for CFRP repair of Class 2 and 3 safety related piping. Note that an effective factor of safety is used here to ensure that all known strength reduction factors are required to be accounted separately as discussed in the following section.

In light of the specific application of CFRP repair for nuclear Class 2 and Class 3 safety related piping, the ASME BPV Code Case N-871 (CC N-871), Section 3000 recommends the use of $S_u/10.0$[‡] to determine the allowable design stress, S_h. In this regard, the recommended factor of safety is 10.0 for ASD method which must be multiplied by all strength reduction factors to determine the effective factor of safety as shown below as a sample calculation.

$$\begin{aligned}\left(FS_{eff}\right)_{ASD} &= Factor\ of\ Safety \times All\ Strength\ Reduction\ Factors \\ &= FS \times C_s \times C_\theta \times {}^{\S}C_T \times \lambda \times C \\ &= 10.0 \times 0.84 \times 0.73 \times \mathbf{1.0} \times 0.6 \times 0.55 \\ &= 2.0\end{aligned}$$

Where *FS* is factor of safety (10.0 as per CC N-871, Section 3000), and C_s, C_θ, C_t, λ and C are various strength reduction factors listed in Table 6. Note that the lowest value of each strength reduction factor is used in the above calculation to capture the worst-case scenario. For example, C_s= 0.84 and C_θ= 0.73 are taken for strength reduction factors due to variation in statistical analysis and effect of misalignment angle, respectively. The material adjustment factor of 0.55[**] for lap shear strength (when exposed to water at 140 F for 50 years of service) causes the potential worst-case scenario. Time effect factor of 0.6 for sustained loading for 50 years of service is used in the calculation. Note that the effect of multi-ply laminate has not been included in the above calculation as this is accounted for separately in determining the ultimate strength of multi-ply laminate using CC N-871, Section 3131 (e).

[‡] $S_u/13.0$ for flexural loading only, i.e. factor of safety is 13.0 for flexural loading as per CC N-871

[§] Note: Tensile tests at elevated temperatures are ongoing and temperature effect factor, C_t will be determined from those tests. At this time, C_t is taken as unity to perform the design calculation.

[**] Even though C=0.45 for flexure is the lowest value, it does not cause the worst condition as FS is 13.0 for flexural loading, i.e. 10×0.55 (lap shear) <13×0.45 (flexure)

As seen in the above calculation, the FS_{eff} is computed to be 2.0 for CFRP repair for 50 years of service life which is less than the required FS_{eff} of 3.5 –and therefore may be non-conservative. Moreover, the effect of temperature has not been included in the calculation. It should also be noted that ASME BPV Code, Section III, Division 1, NC/ND-3600 permits allowable stress multipliers to be used for piping stress evaluations for other Service Levels (upset, emergency, faulted, or service levels, B. C, D) and for secondary stress evaluations that further reduce the effective factor of safety.

To achieve the required FS_{eff} of 3.5 for CFRP repair for 50 years of service life, the recommended *FS* of 10.0 in CC N-871 should be increased to 18.0 as shown below. However, the suggested *FS* of 18 used in the above FS_{eff} equation may need to be adjusted when temperature effect data and worst-case material adjustment factors are available from the other related NRC project.

$$\left(FS_{eff}\right)_{ASD} = \mathbf{18.0}\times 0.84\times 0.73\times \mathbf{1.0}\times 0.6\times 0.55 > 3.5$$

5.1 Impact of Results on Current Version of Code Case N-871

The above discussion on the effective factor of safety has been communicated to the ASME BPV Task Group repair by CFRP (TG-CFRP) since the inception of this project in 2016. Since 2018 the experimental results discussed in Section 3 and Section 4 have been presented to TG-CFRP when they become available after NRC staff review. As indicated above, a summary of the results was also presented at an NRC Public Meeting held on January 16, 2020 [26]. Based on those discussions and experimental results, members of TG-CFRP have decided to revise the design section (Section 3000) of CC N-871 to include some of the strength reduction factors. In the recent (November 2020) version of draft CC N-871-1, the LRFD design method has been deleted in CC N-871 and only the ASD method is provided for designing CFRP repair of safety related piping. Some of the strength reduction factors such as time effect factor (λ), material adjustment factor (C) and effect of temperature (C_T) are now included in the design calculation. These factors are incorporated by reducing the ultimate strength, S_u of CFRP laminate and the recommended factor of safety is 4.0. Following a similar procedure described above, the FS_{eff} per the current draft CC N-871-1 is calculated below. Note that λ, C, C_T and effect of multi-ply laminate are excluded from the calculation as they are included in determining the ultimate strength of CFRP.

$$\begin{aligned}\left(FS_{eff}\right)_{ASD} &= FS \times C_s \times C_\theta \\ &= \mathbf{4.0}\times 0.84\times 0.73 \\ &= 2.45\end{aligned}$$

As seen in the above calculation, the FS_{eff} is computed to be 2.45 for CFRP repair for 50 years of service life which is less than the required FS_{eff} of 3.5 – which may be non-conservative. To achieve the required FS_{eff} of 3.5 for CFRP repair for 50 years of service life, one possible approach would be to use a *FS* of 6.0 (instead of 4.0) or apply C_s and C_θ in determining the ultimate strength of CFRP (and use *FS* of 4.0) as shown below.

$$\left(FS_{eff}\right)_{ASD} = \mathbf{6.0}\times 0.84\times 0.73 = 3.67 > 3.5$$

6. WATERTIGHTNESS TEST

ASME BPV CC N-871, Section I-2400 requires establishing watertightness of the as-designed CFRP repair system through hydrostatic pressurization of cured, full-thickness CFRP repair system. The leak pressure must be at least twice the design pressure. For this purpose, a small-scale watertightness test of the CFRP repair system is conducted using an apparatus specifically designed to conduct the hydrostatic pressurization. Per CC N-871 requirements, the watertightness test could be terminated after achieving twice the design pressure, if there is no leak. The watertightness tests in the current program were continued until the pressure dropped due to the failure of CFRP due to leakage.

Figure 11 shows the watertightness fixture that was designed and built at Emc^2. The dimension of the pressure chamber is 12-in × 12-in at the middle of the fixture. The watertightness fixture should ideally be designed to simulate the actual degraded pipe that would be repaired with CFRP, i.e., the curvature of the fixture should be the same as that of the pipe. However, the current fixture is designed as a flat plate (equivalent to very large diameter) which would provide a conservative estimate of the watertightness pressure for the actual pipe with smaller diameter per the equation given in CC N-871 (Section I-2440 b).

Watertightness panels were fabricated following the same layup configuration as that planned for the full-scale hydrostatic test, i.e., 1D+1H+1L+1W+1H where dielectric layer was facing the top fixture and the 2nd hoop layer was facing the pressure chamber. A sealant (DYNAFLEX^{TM} SC) was used between the watertightness panel and bottom fixture to prevent water leaking through the sides of the fixture. The instrumentation used during the tests include six strain gages to measure strain on CFRP, an LVDT to measure the bulging, pressure transducer, two cameras to record video. A total of three watertightness tests were conducted. However, the sealant on the first test was not cured properly and leaked very early and therefore those data are excluded from this report.

Table 9 shows the watertightness test results where the maximum pressure for Test-2 and Test-3 were 460 psi and 550 psi respectively. In both tests, the watertightness pressure was significantly higher than the minimum requirement of twice the design pressure (2 x 84 psi = 168 psi). However, the onset of leak for Test-2 was through the sealant while the failure mode for Test-3 was a leak through the CFRP system. However, both test specimens showed “river-like” matrix cracking on the Cut-out region as shown in Figure 12. In that regard, Test-3 represents the watertightness pressure more appropriately which showed higher watertightness pressure than Test-2. A summary video of Test-3 watertightness test is also attached with the report. As discussed later, the failure mode for Test-3 was very similar to the failure mode observed in the full-scale hydrostatic test.

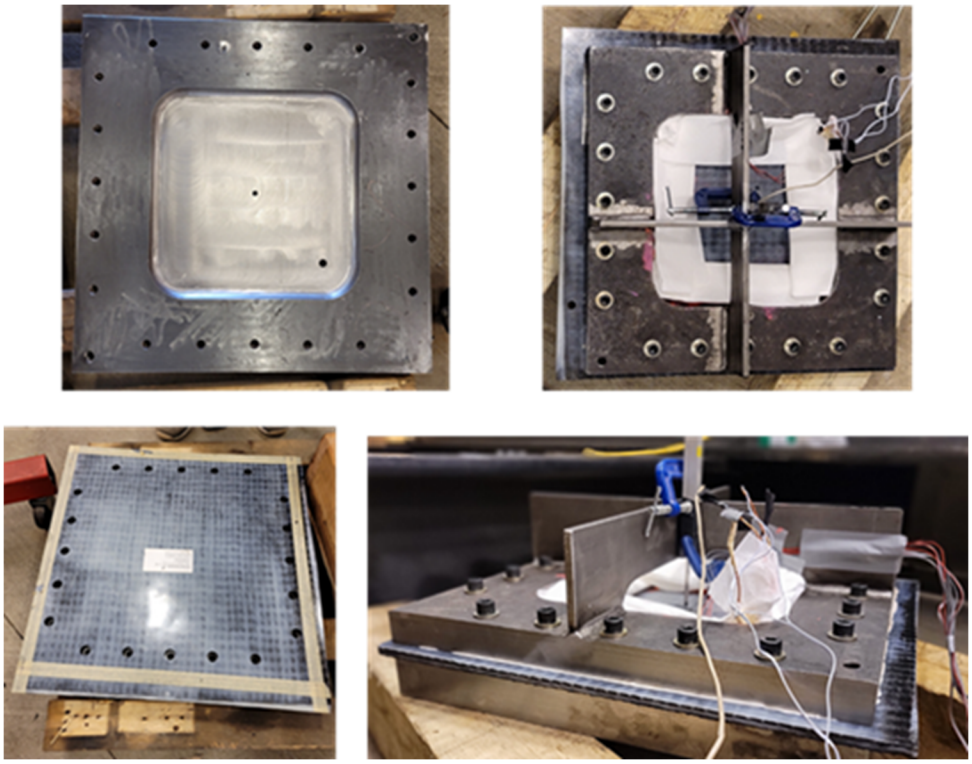

Figure 11 The watertightness fixture built a Emc²

Table 9 Watertightness test results

Watertightness Test ID	Watertightness Pressure, psi	Failure Mode
Test-2	460	Leak through the sealant
Test-3	550	Leak through the CFRP repair system

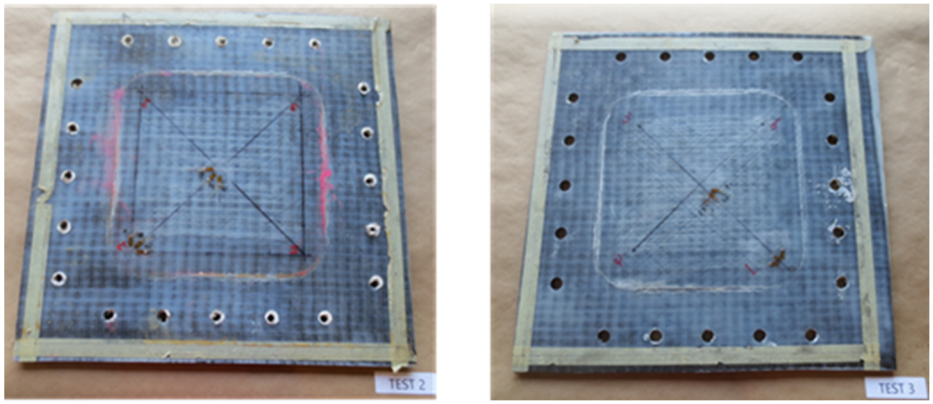

Figure 12 The watertightness test panels showing matrix cracking after test

7. FULL-SCALE HYDROSTATIC TEST OF THE CFRP REPAIR SYSTEM

As discussed above, the CFRP repair is a first-of-a-kind system for use in Class 2 and Class 3 safety-related piping at commercial nuclear power plants. To date, the NRC has approved CFRP repair relief requests at Surry, and is also reviewing other applications on a case-by-case basis. However, prior to approval of the proposed CC N871-1 for blanket approval of CFRP repairs, it was considered essential to conduct an independent full-scale test of such a repair to confirm the design basis and the safety margins involved. Therefore, after extensive discussions with NRC staff the first full-scale hydrostatic test of a large diameter steel pipe with a significant "defect" repaired per the above Code Case was planned and conducted at Emc^2 as detailed below.

The full-scale hydrostatic test was conducted at room temperature (72 F) under *short-term loading* to evaluate the available margin for Class 2 and 3 degraded piping repaired with CFRP as per ASME BPV CC N-871. A 40-inch diameter degraded steel pipe with 0.375-inch wall thickness was used to design this test. A 12-inch × 24-inch cut-out hole was machined in the pipe to represent one of the worst-case scenarios of corrosion defects repaired by CFRP as per CC N-871. The details of the test design, CFRP repair design calculations, CFRP repair installations and full-scale hydrostatic test are described in the following sections.

7.1 The Full-Scale Hydrostatic Test Design

The full-scale hydrostatic test was designed such that it would represent a key design condition involving a significant defect in-service piping, and yet ensured that the test could be carried out safely indoors in Emc^2's structural and materials testing laboratory. The short-term loading case was used as one of the design conditions for the test at a working pressure of 84 psi and at room temperature (72 F). The short-term loading indicates that the CFRP repair materials have not been subjected to any long-term materials property degradation such as exposure to harsh environment (water, salt-water, etc.) or creep due to sustained loading discussed above. Also, since this hydrostatic test was designed to be conducted at room temperature, the effect of elevated temperature is not investigated in this experiment.

A 40-inch diameter carbon steel pipe with 0.375-inch wall thickness was used to design the test. Since the CFRP repair is always designed to take the entire load, that is, the degraded host pipe is assumed to carry no load whatsoever, a through-wall cut-out in the steel pipe was used as an "artificial flaw" for the test representing one of the worst-case scenarios of corrosion defects. To facilitate designing the optimal flaw dimension, a 3D finite element (FE) model of full-scale pipe with CFRP repair was first created using ABAQUS®. The FE model was then used to analyze three flaw dimensions to investigate which flaw dimension provided the highest loading scenario for CFRP repair while restricting the stresses in the host pipe to below the yield strength to ensure that the test is conducted safely. Figure 13 shows one of the FE models (half-symmetry) with a cut-out and CFRP repair system and Figure 14 shows three flaw dimensions used in the FE model with same width (12 inch) in the axial direction but varying length in the circumferential directions such as i) about 20% of the circumference, ii) 50% of the circumference and iii) 100% of the circumference, i.e., two pieces of pipe. *Note that this FE model was developed to facilitate the pre-test design, and not a predictive tool since it does not include any damage model for the CFRP or steel.*

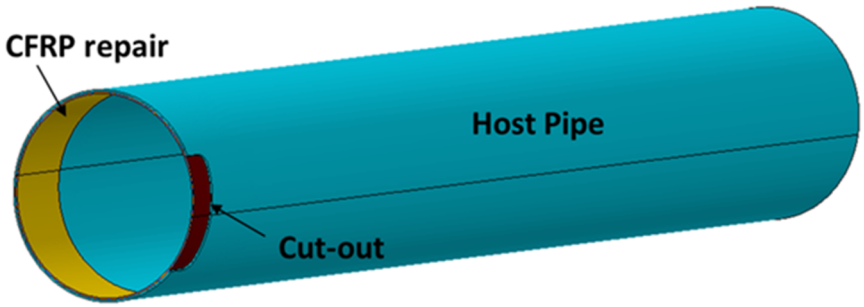

Figure 13 3D finite element model (half-symmetry) of full-scale pipe with a cut-out and CFRP repair

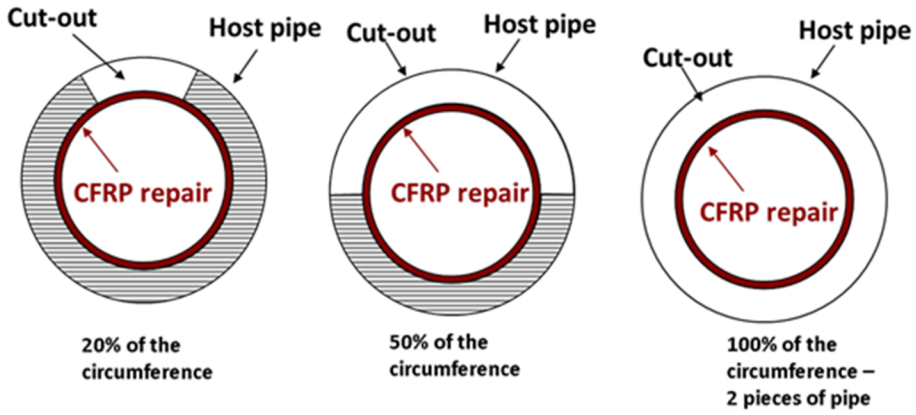

Figure 14 Three flaw dimensions for FE model

Elastic-plastic FE analyses were conducted for two flaw sizes, 20% and 50% of the circumference with CFRP repair of up to 500 psi internal pressure to evaluate the stresses in the steel host pipe. Figure 15 shows the hoop and the longitudinal stresses in the steel host pipe indicating a high stress area near the corner of the cut-out due to stress concentration. As seen in the figure, longitudinal stresses for both flaw sizes are lower than the nominal yield strength of 70 ksi of the pipe material. However, the hoop stress for the flaw size of 50% of the circumference is higher than the yield strength of the pipe while it is lower for the smaller flaw size. *These FE analyses confirmed that a flaw size as large as 20% of the circumference could be used in the host pipe to conduct the hydrostatic test and yet restrict the pipe stresses to below yield strength value to meet safety considerations in the laboratory*. The next set of FE analyses were performed to investigate how the stresses and strains in CFRP layer varied with the flaw size. As per design limit stated in CC N-871, shear stresses in the adhesive between steel pipe and CFRP repair system, and hoop strains in the CFRP layers are some critical parameters and are shown in Figure 16 and Figure 17 for three flaw sizes. As seen in Figure 16, hoop shear stresses in the adhesive between steel pipe and CFRP repair for 20% and 50% of the circumference dominate all stresses and their maximum values are similar (around 2 ksi). On the other hand, axial shear stress in the adhesive is dominant for the flaw size of 100% of the circumference with a maximum value of only 0.36 ksi – much lower than that for the other two flaw sizes. Maximum hoop strains in the hoop layer of CFRP repair system are very similar (0.51% – 0.57%) for all three flaw sizes as shown in Figure 17. These FE analyses suggest that due to the stress concentration around the corner of the cut-out, the case with the flaw size of 20% of the circumference will cause a similar or higher loading

in CFRP repair system as the other larger flaw sizes. The aforementioned FE models were also used to choose the length of the pipe. It was found that a 13-ft long pipe would be adequate to avoid any end-effects during the hydrostatic test. *Based on the above FE analyses, a flaw size of 12-inch axial length and 24-inch circumferential length corresponding to about 20% of the circumference was chosen for the hydrostatic test with total pipe length of 13 ft.*

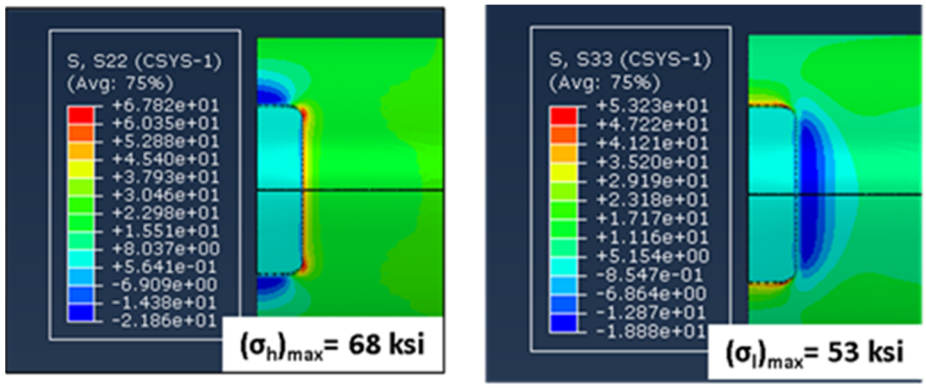

(a) Flaw size: 20% of the circumference

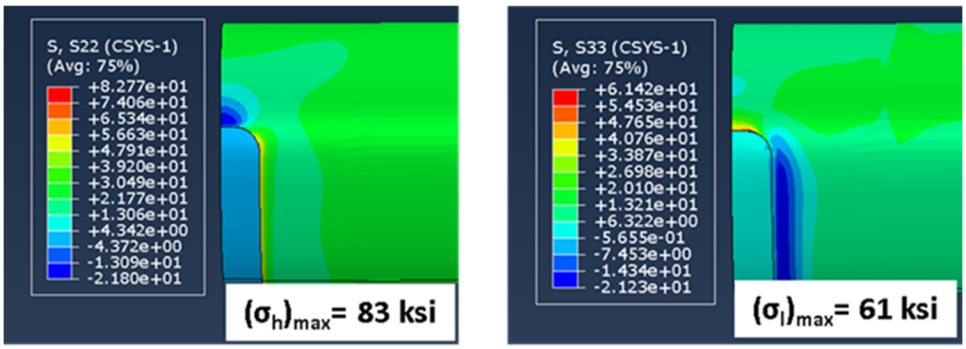

(b) Flaw size: 50% of the circumference

Figure 15 Hoop and longitudinal stresses in the steel host pipe under 500 psi internal pressure

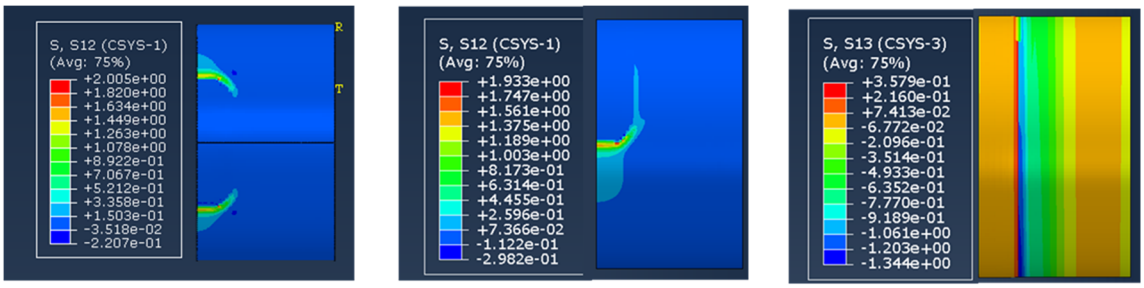

(a) 20% of the circumference (b) 50% of the circumference (c) 100% of the circumference

Figure 16 Shear stresses in adhesive between steel host pipe and CFRP repair under 200 psi internal pressure

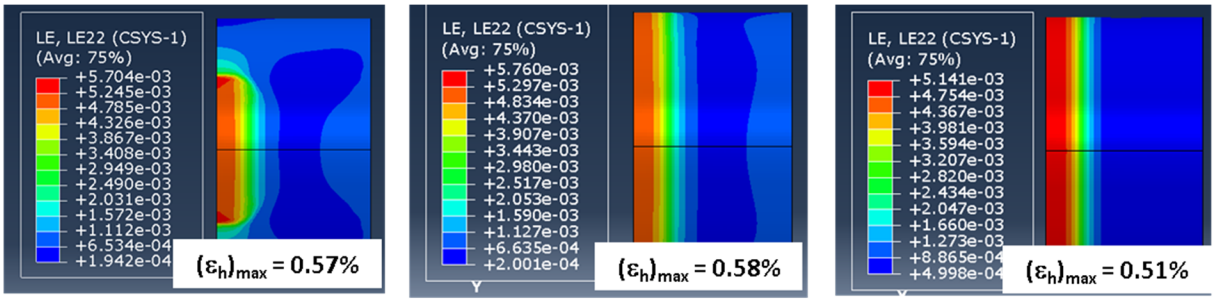

(a) 20% of the circumference (b) 50% of the circumference (c) 100% of the circumference

Figure 17 Hoop strain in CFRP hoop layer under 200 psi internal pressure

7.2 Design Calculation of the CFRP Repair System

Design calculations of the CFRP repair system were conducted according to CC N-871 where a factor of safety (FS) of 10.0 and 4.0 on the characteristic value of the ultimate strength of CFRP laminate and shear strength of the epoxy respectively were applied. These calculations showed that the recommended design pressure for the full-scale test would be 84 psi[††]. However, as will be discussed in later section, the full-scale hydrostatic test was conducted beyond the design pressure until failure occurred. The input parameters for design calculations are given in Table 10. As per this design calculation, the required number of CFRP layers in hoop and longitudinal directions are 2 and 1 respectively with a terminal end length of 6 inches on both sides of the flaw. Therefore, the total length of each layer is 24 inches (12 inches flaw + 6 inches terminal end on both sides of the flaw). The detailed design calculations are provided in Appendix C. Additionally, CC N-871 requires one layer of dielectric GFRP and one watertightness GFRP layer. The final configuration of the CFRP repair system for the test is given below.

1D + 1H + 1L + 1W + 1H

Where D is GFRP dielectric layer, H is CFRP hoop layer, L is CFRP longitudinal layer and W is GFRP watertightness layer.

Table 10 The input values for design calculation of the CFRP repair system

Characteristic value of the tensile strength	152.2 ksi
Characteristic value of the tensile modulus	12,312 ksi
Weibull mean value of the tensile modulus	14,163 ksi
Shear bond strength of CFRP on host pipe	1,100 psi
Length of terminal ends	6 inch

[††] As composite layup is a discrete system, the number of required layers is typically rounded to the next whole number in actual service condition to add conservatism. However, in the current project, the exact design pressure of the mock-up test was iteratively calculated to be 84 psi.

7.3 Installation of CFRP Repair System

The installation of the CFRP repair system was done by Structural Technologies Inc. and SGH at Emc^2's laboratory where the hydrostatic test was performed. These vendors were selected since they had installed the only CFRP repair for a safety-related system at the Surry nuclear power plant. A 12-inch axial length and 24-inch circumferential length cut-out was machined at the center of the axial length of the pipe where all four corners were rounded with 2-inch radius curvature as shown in Figure 18. All edges of inside surface of the cut-out were also rounded to avoid sharp corners pinching on CFRP repair surfaces. A backing steel plate with release film was also made as shown in Figure 18 (b) which was used to support the CFRP layup during installation. The backing plate was removed after installing the first layer. The following sections discuss key steps during installation along with details of the curing temperature, degree of curing and glass transition temperature and the results of the witness panels. Several NRC staff were originally planning to visit Emc^2 to witness the installation procedure and the test. However, due to the COVID-19 pandemic and travel restrictions, the whole installation procedure was live streamed to NRC staff via multiple cameras instead.

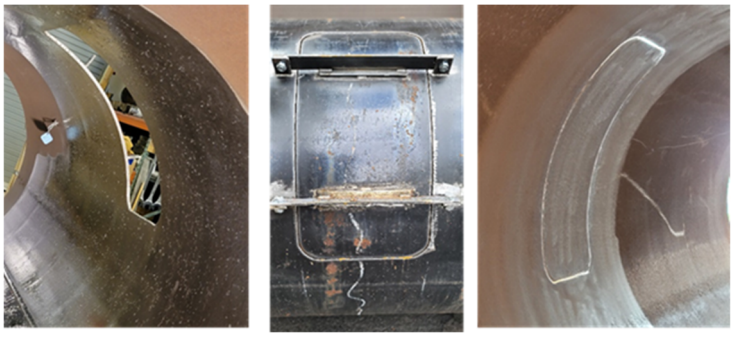

(a) (b) (c)

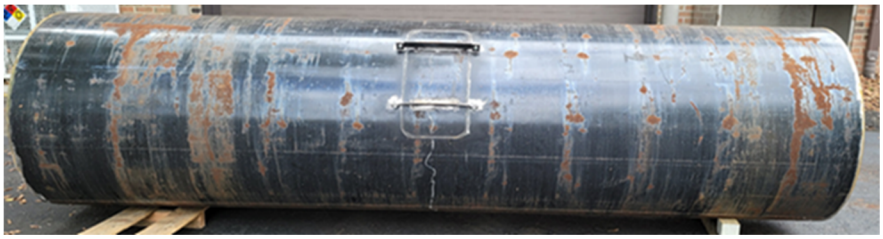

(d)

Figure 18 The test pipe with 12″ × 24″ cut-out before CFRP installation

7.3.1 Key steps during installation

While the detailed report of the installation procedure as provided by Structural Technologies Inc. is given in Appendix D [CONTAINS PROPRIETARY INFORMATION], a brief description of the key steps during installation is provided here. The materials used for CFRP repair system are V-Wrap™ C400HM as unidirectional carbon fiber, V-Wrap™ EG50-B as bi-directional glass fiber and V-Wrap™ 770 Epoxy (see Appendix A for MSDS and Technical Data Sheets). Per the design calculation in Section 7.2, the layup configuration for CFRP repair system was (1D+1H+1L+1W+1H) where dielectric and watertightness layers were bi-directional GFRP, and hoop and longitudinal layers were unidirectional CFRP. The total nominal fiber thickness of the

CFRP repair system was 0.308 inch and the total length of the repair was 24 inches including the 6-inch terminal length on either side of the cut-out.

A high-level overview of the CFRP repair installation procedure is shown as a flow diagram in Figure 19. Note that this flow diagram only shows the high-level installation process which does not include in-process inspection, quality control inspection, witness panel testing etc. The detailed flow diagram is given in Appendix D. Key steps are briefly described below and the photographs are shown in Figure 20.

1. After visually inspecting the host pipe to remove any sharp edges, weld irregularities, rust etc., sand blasting (Figure 20a) was used to prepare the inner surface (Figure 20b) of the host pipe repair area (including the backing plate) as per design requirements. Adhesion tests were performed on as-prepared surface to ensure that it met the design requirement.
2. A thin layer of epoxy primer was then applied on the inner surface of the host pipe to provide sufficient adhesion between host pipe and composite layups (Figure 20c).
3. Epoxy components were then mixed according to Technical Data Sheets and each fiber fabric was saturated in a mechanical saturator just before the installation (Figure 20d). Weight ratio test was performed to ensure the correct amount of epoxy was applied.
4. Thickened epoxy (fumed silica mixed with epoxy to create a trowel-able consistency for application to the host pipe) was applied on top of the primer followed by the dielectric GFRP layer. Subsequently, the remaining CFRP and GFRP layers are applied with a layer of thickened epoxy between each layer. Note that only two layers were applied per day such as dielectric GFRP and 1st CFRP hoop layer were installed on Day 2 followed by longitudinal CFRP and watertightness GFRP on Day 3 and 2nd CFRP hoop layer on Day 4 (Figure 20e - Figure 20h). After each day of installation, the repair was cured at around 85 F using a space heater inside the pipe until starting the next day of installation.
5. Another layer of thickened epoxy was applied as top coat followed by the installation of two expansion rings on either end of the CFRP repair system (Figure 20i).
6. After installing the top coat, the whole repair system was post-cured at around 85 F for two days (Figure 20j) after which Differential Scanning Calorimetry (DSC) samples were collected from three locations to determine the degree of curing.

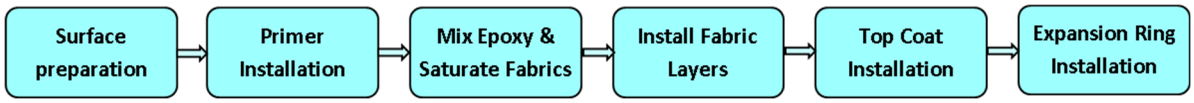

Figure 19 The high-level CFRP repair installation process flow diagram

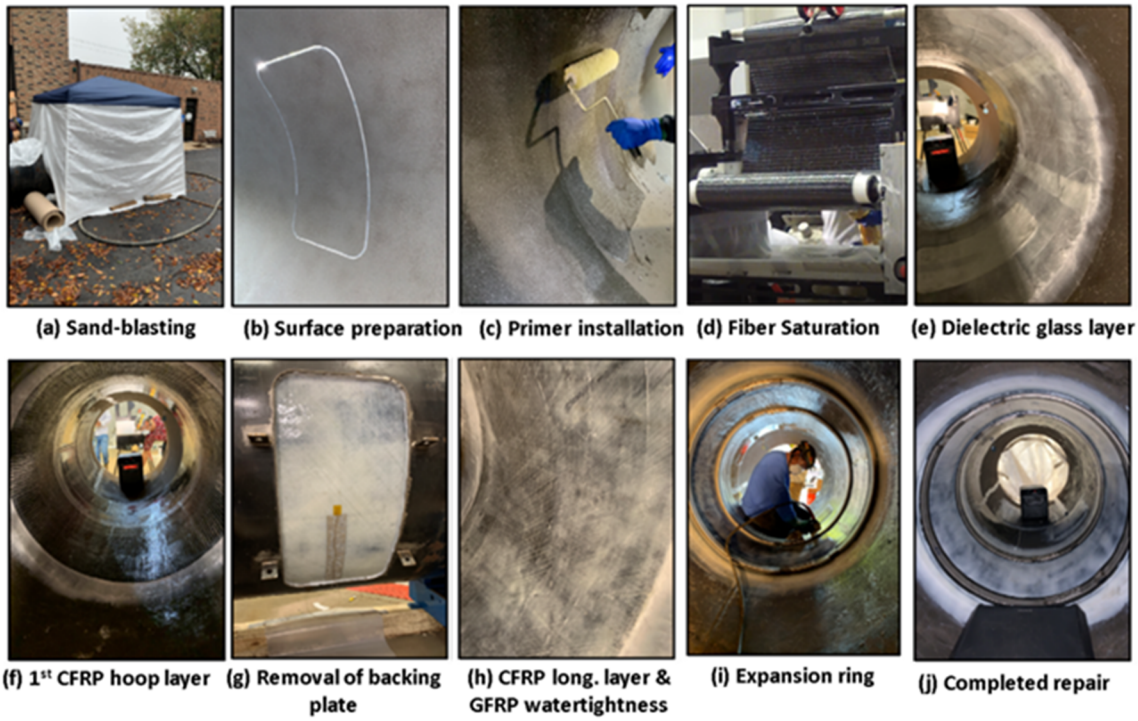

Figure 20 The key steps in CFRP repair installation process

7.3.2 Some other steps during installation

In addition to the key steps described above, Figure 21 shows some additional items of interest which are briefly described below.

- The expansion rings consist of a stainless-steel ring, shims and an ethylene propylene diene monomer (EPDM) rubber strip were placed onto CFRP repair system at both terminal ends and were expanded using hydraulic expander as per design requirements (Figure 21a). The detailed installation is given in Appendix D.
- Figure 21b shows the weight ratio test machine where each saturated fabric was tested to ensure that the correct amount of epoxy was applied in each layer.
- Figure 21c shows how the ends of each composite layer overlap after wrapping 360° around the circumference. Thickened epoxy was applied on top of each layer before installing the next layer which provided a smooth surface over the overlap area.
- Figure 21d shows the location of witness panel which was installed away from the repair area after preparing the surface of the host pipe. Pull-off tests were conducted on this panel to ensure that the adhesive strength met the design requirements.
- Figure 21e shows the location of witness panel that was installed per Emc^2 guidance (not required by CC N-871). This witness panel was installed to monitor the curing temperature during installation. Emc^2 personnel installed one thermocouple on top of each layer (total of five layers) including one on the pipe, one on the top coat. These thermocouples were installed to investigate how the curing temperature varies for each composite layer as the curing progressed over 7 days.

- Figure 21f shows another thermocouple installed at the center of the cut-out on the inner-most epoxy layer.

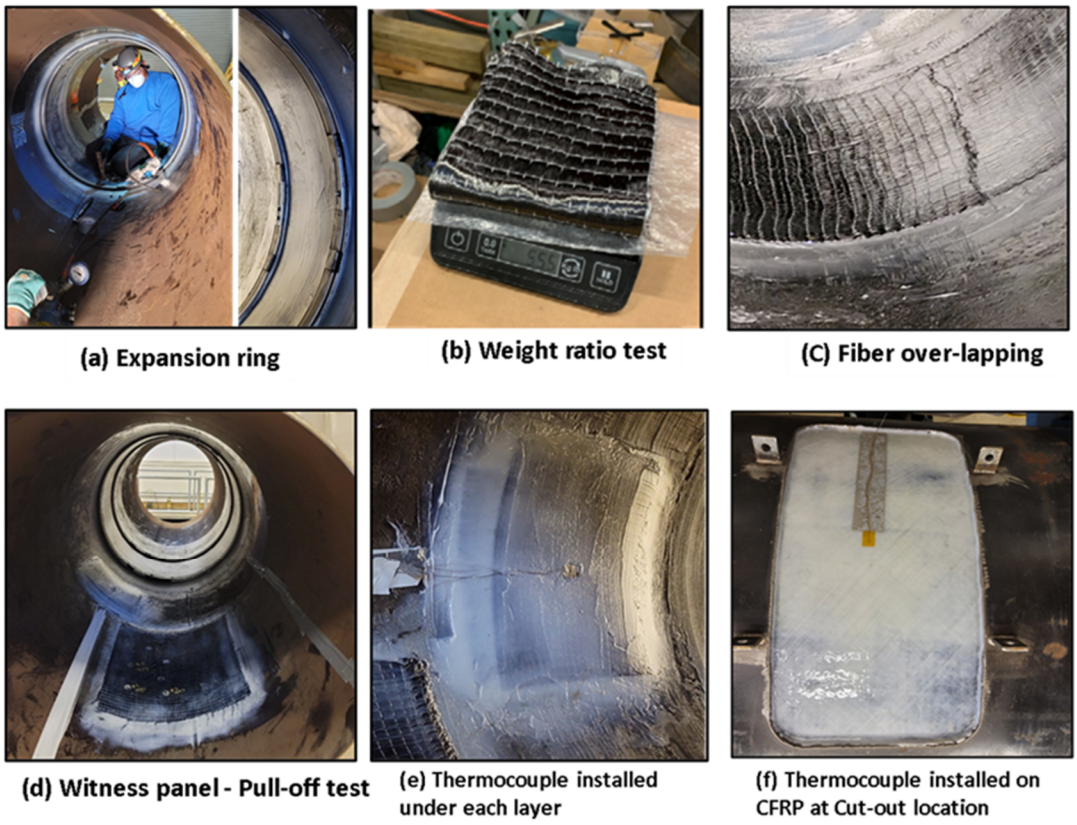

Figure 21 Some other steps in CFRP repair installation process

7.3.3 Curing and post-curing temperatures during installation

Curing and post-curing temperatures were monitored in two ways – 1) using two temperature/humidity data loggers installed by the CFRP installer, and 2) using thermocouples placed under each layer of composites installed by Emc^2 personnel as shown in Figure 22. A space heater inside the pipe was used to cure and post-cure the CFRP repair system.

Two temperature/humidity data loggers were located inside the host pipe on either side of the CFRP repair as shown in Figure 22(a). The data loggers were suspended from the inside surface of the pipe that measured the air temperature over the entire period of curing and post-curing as shown in Figure 23. As seen in Figure 23, both curing and post-curing temperatures range between 85 F and 95 F on either side of the CFRP repair system over the entire period of curing and post-curing. Note that the heater was removed during installation of each layer as indicated by the sudden drops of temperature during "installation and curing" process.

To monitor how the curing and post-curing temperatures vary for each composite layer over the entire period of curing and post-curing process, thermocouples were installed under each layer of composite layer by Emc^2 personnel (Figure 22b). Thermocouples were also installed on the pipe surface, top coat and cut-out window on the outside surface. Figure 24 shows the temperature data from all eight thermocouples installed under each layer of CFRP repair. *The main take away*

from this figure is that the range of curing temperatures among all composite layers are quite close to each other for any particular day suggesting that heat had been transferred reasonably through all composite layers and hence, all layers should experience similar curing condition. However, it should be also noted that the length of the test pipe (13-ft) and CFRP repair (2-ft) were relatively short as compared to long pipe and a repair installed under field conditions. During post-curing for 2 days, the temperature range on all composite layers, host steel pipe and top coat was within 4 F (between 83 F to 87 F). As may be noted in Figure 23, the thermocouple installed on the cut-out window outside the pipe on the inner-most layer of epoxy showed relatively high temperature (~120 F) on the 3rd day of curing as compared to other layers. After discussion with the installer, it was believed that a space heater placed outside the pipe may have been blowing directly on that particular thermocouple causing this anomaly. However, this did not affect the curing of the remaining layers as evident from the DSC results discussed in a later section.

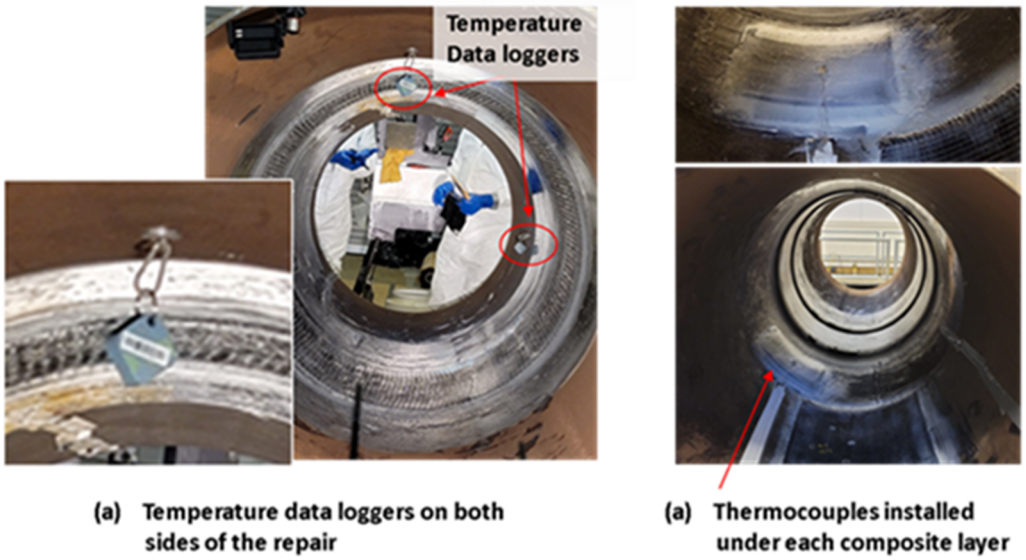

Figure 22 Temperature data loggers and thermocouples installed to monitor curing and post-curing temperatures

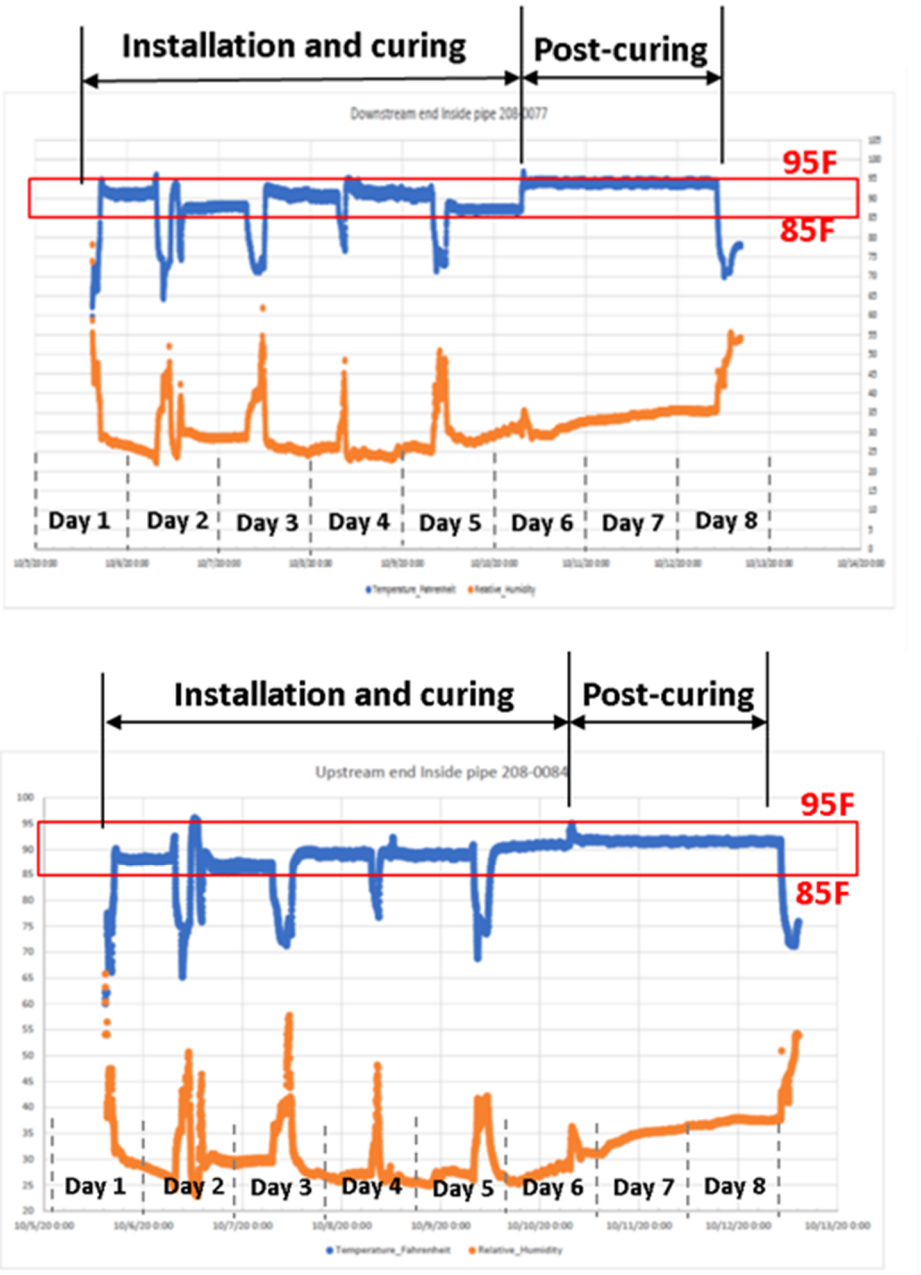

Figure 23 Temperature and relative humidity data from the data loggers over entire period of curing and post-curing

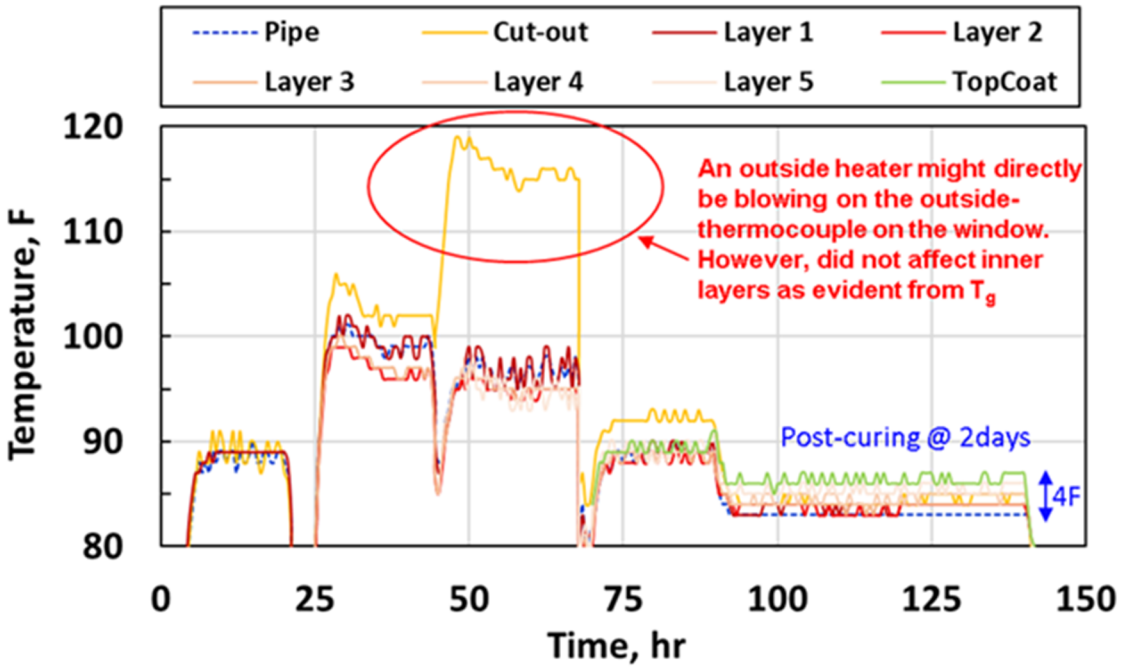

Figure 24 Temperature data from thermocouples installed under each layer of CFRP repair system over entire period of curing and post-curing

7.3.4 Degree of curing and glass transition temperature (T_g)

After post-curing for 2 days at around 85 F, three DSC samples were collected from three locations: Cut-out ID, Host Pipe ID from terminal end, and Cut-out OD. Samples were sent to SGH to run DSC on these samples as part of their installation procedure. DSC tests were conducted according to ASTM E2160-04(2018) using a PerkinElmer Sapphire Differential Scanning Calorimeter (DSC) which heated one sample at a time from an initial temperature of 20 C to a final temperature of 350 C at a rate of 20 C/min. Nitrogen purge gas was used at a flow rate of 200 mL/min. SGH reported that all three samples achieved more than 89% of curing meeting the CC N-871 requirement of achieving a minimum of 85% curing (see Table 11). The heat flow versus temperature curves from DSC tests for three samples are given in Figure 25 (high resolution figures are given in Appendix D, Attachment D1, page 144-146) which were used to determine heat of cure to evaluate the degree of cure by comparing against a calibrated heat of cure. As a part of the installation procedure per CC N-871 recommendation, the user only needs to evaluate the degree of curing. However, as discussed previously, the glass transition temperature (T_g) of epoxy also needs to be evaluated to ensure that the T_g is higher than the maximum design temperature by a minimum specified value amount (CC N-871 currently suggests this value to be 40 F; confirmatory tests are ongoing on the related NRC project to verify this value). Emc^2 conducted an independent analysis of DSC results shown in Figure 25 to estimate the T_g for these three samples. As seen in this figure, T_g for specimens collected from "Cut-out ID" and "Host pipe ID" are very similar (122 F-145 F) and within the range of 140 F for 85 F curing temperature. Whereas T_g for specimen from "Cut-out ID" was higher (144 F-176 F) which may be attributed to the higher curing temperature (120 F on Day 3 curing as shown Figure 24). Note that each DSC results showed a peak around the T_g area which may be attributed to heat relaxation. However, the presence of these peaks made the determination of T_g difficult.

Table 11 Degree of cure and glass transition temperature (T_g) of CFRP repair system

Samples	Heat of Cure, (J/g)	Degree of Cure (%)	T_g (C)	T_g (F)
Cut-out ID	-31	92	50-62	122-144
Host Pipe ID	-44	89	50-63	122-145
Cut-out OD	-14	97	62-80	144-176

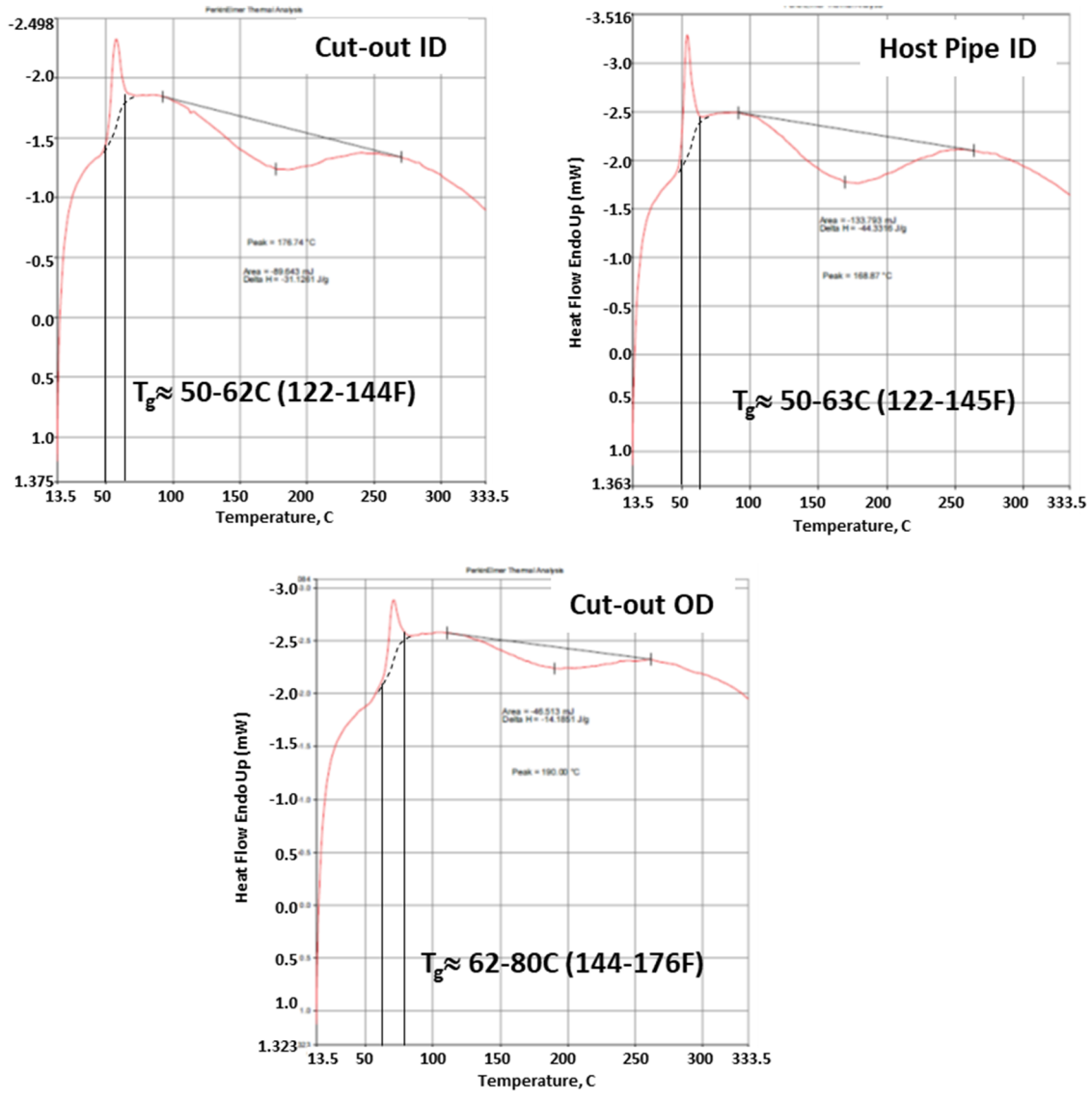

Figure 25 DSC results for three samples collected from CFRP repair system of the test

7.3.5 Results of witness panels

7.4 Performance of the Hydrostatic Test

7.4.1 Hydrostatic test setup and instrumentation

Figure 26 shows the schematic of the full-scale hydrostatic test of a 40-inch diameter 13-ft long steel pipe with a 12-in × 24-in hole at the center of the axial length of the host pipe which was repaired by CFRP system with 24-inch length as per ASME BPV CC N-871 as described previously. Photographs of various steps during the test setup are shown in Figure 27. As seen in Figure 26 and Figure 27, two volume absorbers, each 30-inch diameter and 4-ft long were inserted inside the test pipe to reduce the energy release in the event of any catastrophic failure during the test. The volume absorbers were placed on either side of the repair and were welded to each end of the host pipe to restrict them from moving as shown in Figure 27. After securing the volume absorbers, two end-caps were welded on either side of the host pipe as shown in Figure 27. The test pipe was secured inside a test pit with strong I-beam structure inside the Emc^2 laboratory and a protective shield (made of large diameter steel) was secured over the test pipe for additional safety during the hydrostatic test, see Figure 27 and Figure 28.

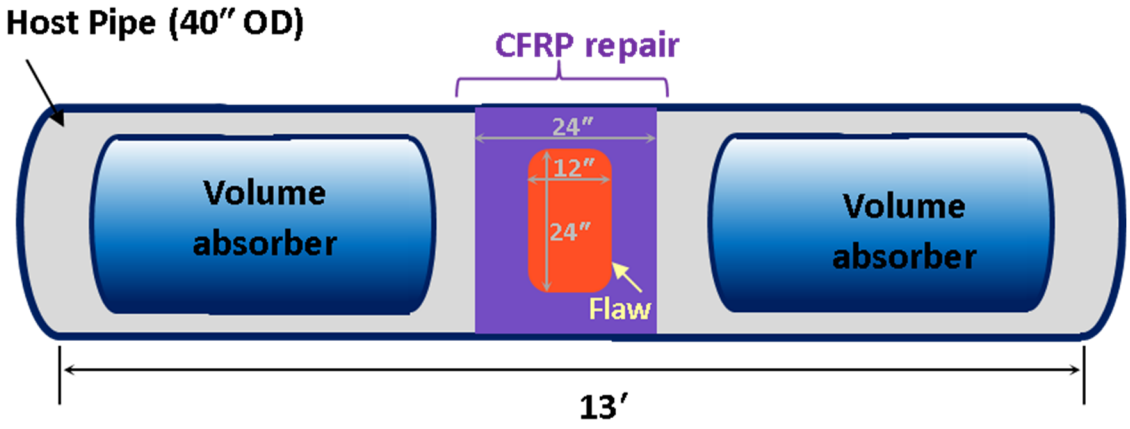

Figure 26 Schematic of the full-scale hydrostatic test setup

Figure 28 shows the detailed instrumentation installed on the host steel pipe and CFRP repair system. There was one pressure transducer, one LVDT on the CFRP at the center of the cut-out measuring the bulging of CFRP system and one thermocouple at the cut-out location measuring the test temperature. There were 15 strain gages mounted on CFRP – 3 strain gages forming a triaxial set on each of four corners of the cut-out and another triaxial set at the center of the cut-out on CFRP. Each triaxial set was placed to measure hoop, longitudinal and 45° strains on CFRP. The 3 strain gages forming a triaxial set were mounted on the steel host pipe at one of the corners of the cut-out. The strain values from these strain gages were monitored live during the test to ensure the strain on the pipe material would not exceed the yield strain. Four cameras and LED light strips were installed underneath the shield to record the video covering the whole area of the cut-out and instrumentation. Several NRC staff were originally planning to visit Emc^2 to witness the full-scale hydrostatic test. Due to COVID-19 pandemic and travel restrictions, the entire full-scale hydrostatic test was live streamed to NRC staff via multiple cameras.

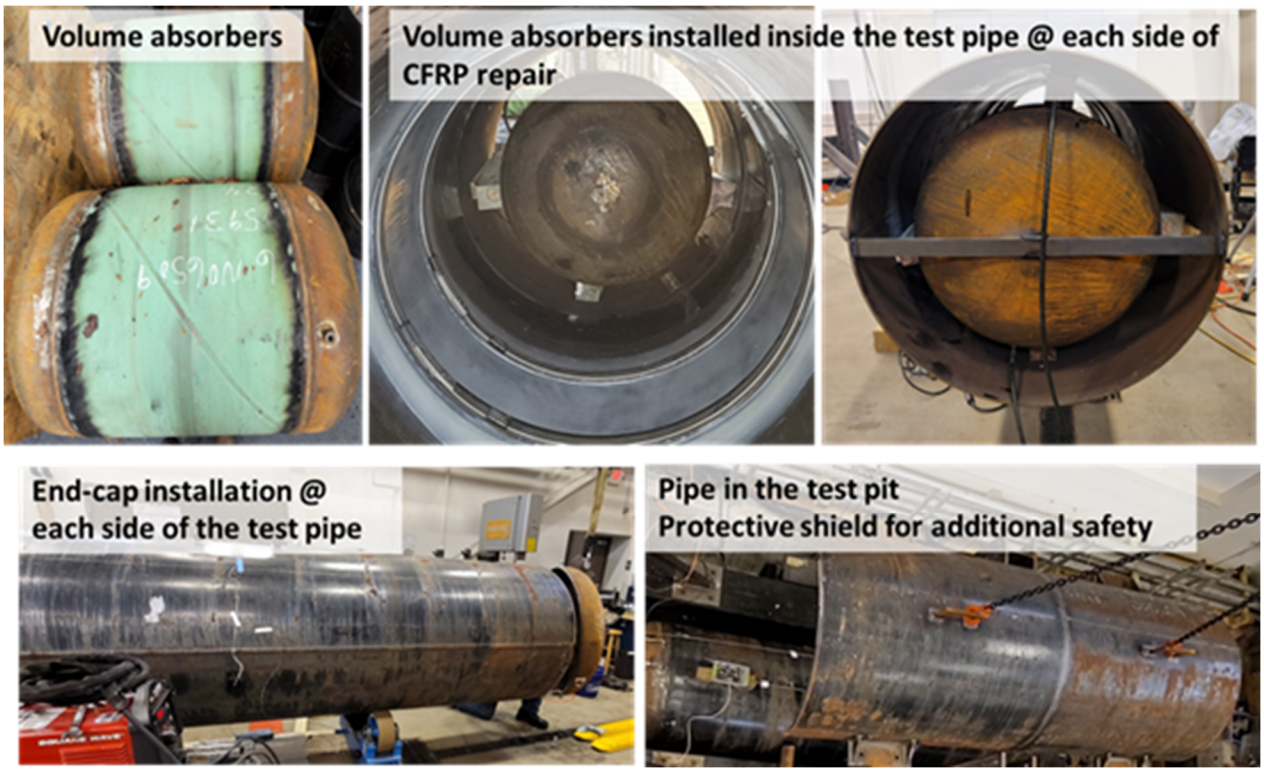

Figure 27 Photographs showing various steps of the test setup

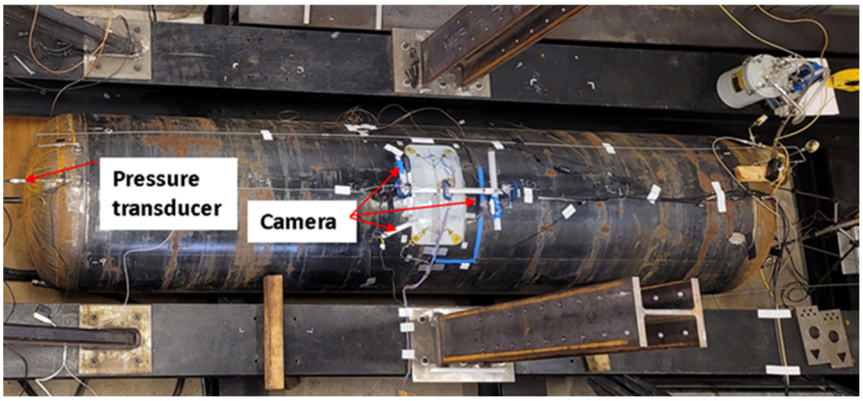

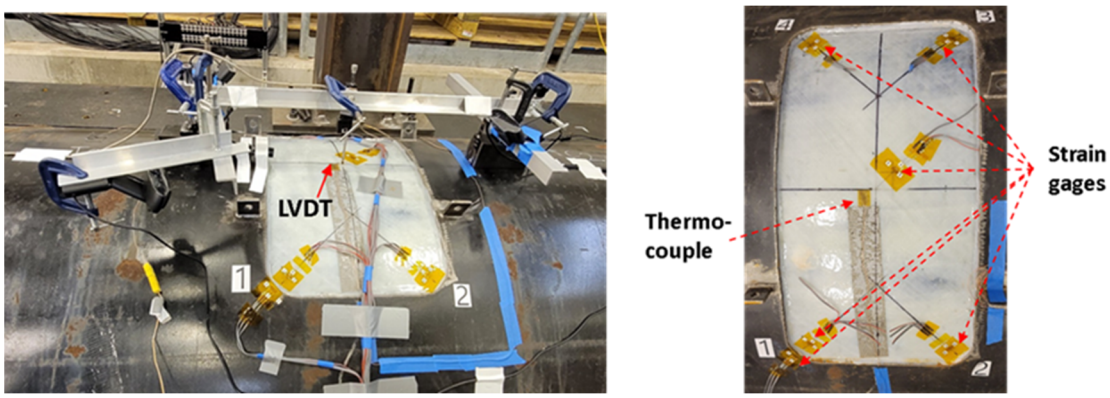

Figure 28 Instrumentation for the full-scale hydrostatic test

7.4.2 Hydrostatic test results

The hydrostatic test was conducted in the test pit inside Emc^2 laboratory in a conditioned environment at room temperature (72 F). The test pipe was filled with water and left inside the test pit for a few days to reach steady-state room temperature (72 F). The test pipe was pressurized with stepwise pressure increment such that the pressure was held for at least 10 minutes for every 50 psi increment. Pressure control, data acquisition, video recording/watching and live streaming were monitored from a control room away from the test pit. Strain gage data were monitored live during the test to ensure the host pipe material did not yield as well as to monitor strain level in the CFRP repair system. Video and audio from four cameras were monitored live to see/hear the onset of failure.

Figure 29 shows the pressure versus time plot for the full-scale hydrostatic test which took about four hours to complete. As seen in the figure, the onset of initial leak started at 600 psi after about 168 minutes. At initial failure, a low energy water leak occurred through a small pinhole near the edge of the cut-out between Corner 1 and 4 as shown in Figure 30 (a). After initial leak, the pressure was held at 600 psi (leak pressure) for another 40 minutes when a significant cracking noise in the matrix was heard followed by the observation of several pinhole type leaks in the area between Corner 1 and 2 as shown in Figure 30 (b). At this stage, the pressure started to drop and at around 580 psi, the release valve was opened to quickly drain the water to preserve the failure modes in the CFRP for post-test analysis. This failure was designated as final leakage failure. *The failure mode for the full-scale hydrostatic test with CFRP repair was designated as a "leak" preceded by significant matrix cracking noise, and the failure (leak) pressure for this test was 600 psi.* A summary video of the full-scale hydrostatic test is also attached with the report.

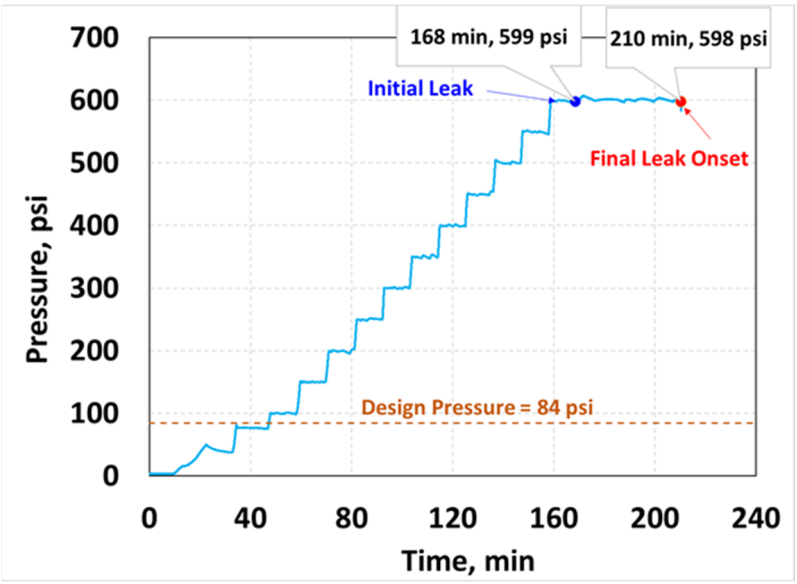

Figure 29 Pressure versus time data from the full-scale hydrostatic test

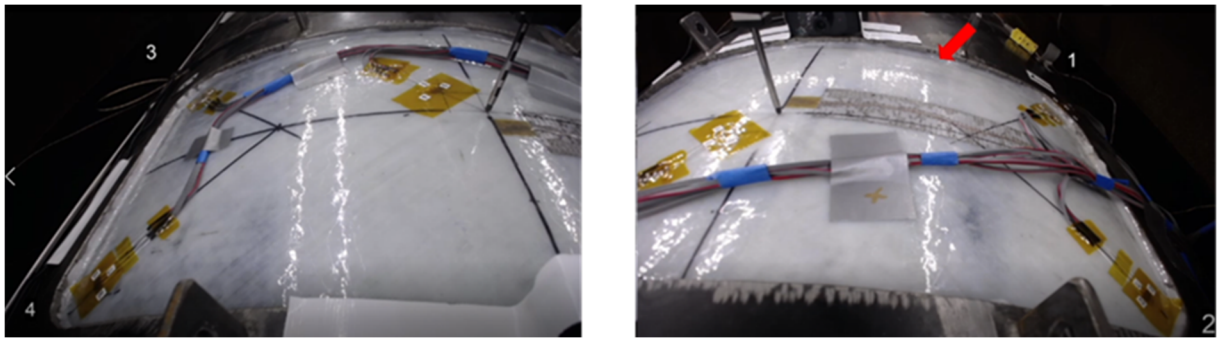

(a) Onset of initial leak

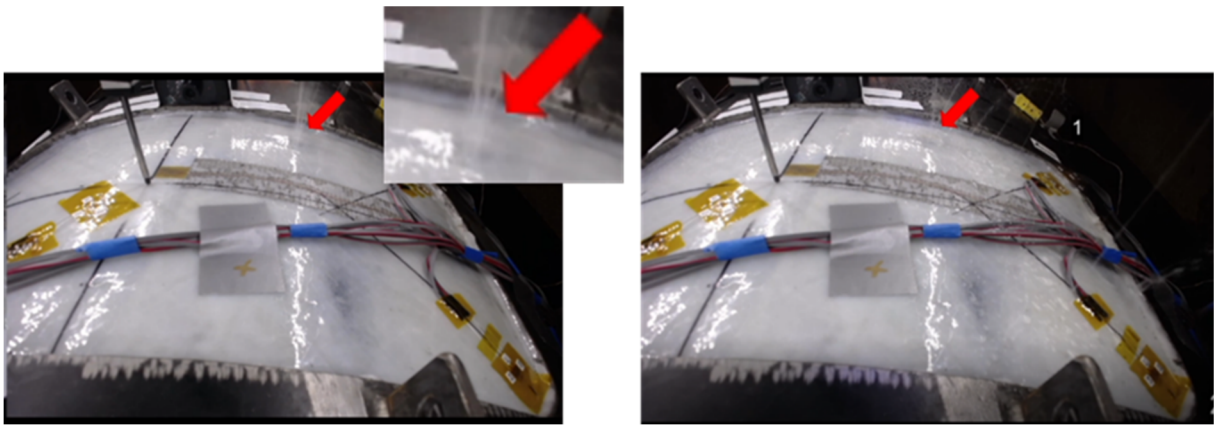

(b) Onset of final leak

Figure 30 Onset of initial and final leak during the hydrostatic test

Failure (leak) pressure of 600 psi in the test is reasonably close to the watertightness pressure (from Test-3) of 550 psi. Note that the watertightness test was conducted using a flat-plate fixture which provided a conservative watertightness pressure. The failure modes for both watertightness test and the test look very similar, i.e., river-like matrix cracking followed by water leaks.

Figure 31 shows the pressure versus bulging data and Figure 32 shows the temperature data during the hydrostatic test. As seen in Figure 31, maximum bulging of the CFRP repair system at the center of the cut-out was 0.13 inch at 600 psi failure (leak) pressure. The test temperature was 72 F for the entire period of the hydrostatic test.

Strain gage data on both host steel pipe and CFRP system as a function of pressure is shown in Figure 33. Figure 33(a) shows the photograph of CFRP repair system through cut-out indicating the locations of initial and final leak as well as the identifications of four corners where strain gages were mounted. Figure 33 (b), (c), and (d) show pressure versus strain plots for host steel pipe and four corners of CFRP in hoop, axial, and 45° directions respectively. As seen in the figure, strain values were less than 0.1% for both axial and hoop directions for steel pipe ensuring that the pipe material did not yield (0.2% yield strain) during the hydrostatic test. Note that one strain gage (45° direction) on the pipe was lost before starting the hydrostatic test. At all four corner locations for CFRP repair system, hoop strains were the largest and dominating with a range of 0.27%-0.33% whereas the axial strains were within a range of 0.17-0.26%. The initiation of leak occurred at a location near Corner 1 (see Figure 30) and final leak occurred in the vicinity of Corner 1 and 2 where the hoop strains (for both Location 1 and 2) were maximum (about 0.33%). These strain data coupled with matrix cacking noise indicate that the matrix of CFRP repair system cracked at a strain value of around 0.33%, potentially creating a leak path through the matrix, CFRP and GFRP watertightness layers. Post-test analysis of the test specimen revealed several river-like cracking marks on the CFRP repair system on the inner or top (from inside the pipe) surface of the CFRP repair system behind the cut-out area (especially near Corner 1 and 2) indicating that the potential failure mode was matrix cracking and hence, leak through the CFRP system (see Figure 34). There was no evidence of water found near the edge at the bonded area between the host pipe and CFRP repair suggesting that the leak did not occur within the bond. Also, no evidence of fiber breakage was noticed at 600 psi leak failure pressure.

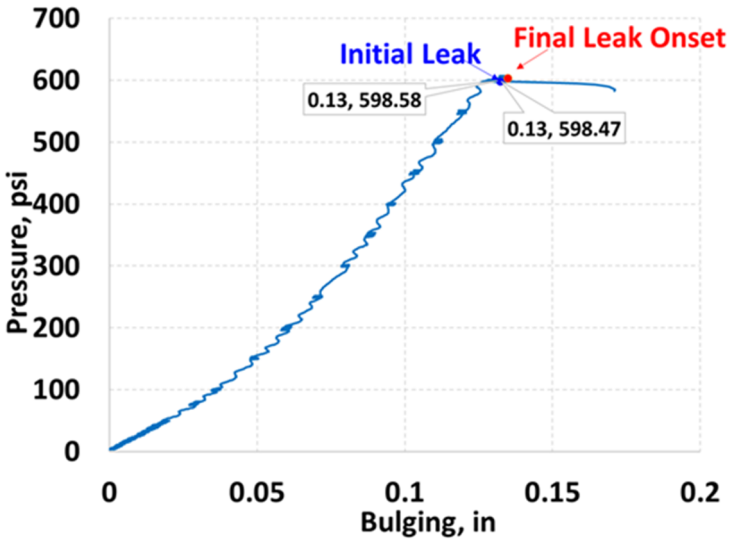

Figure 31 Pressure versus bulging during the hydrostatic test

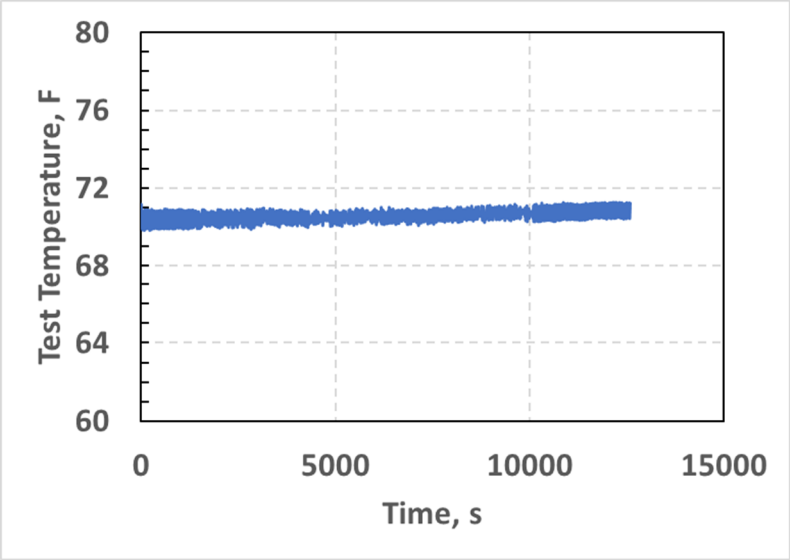

Figure 32 Temperature data during the hydrostatic test

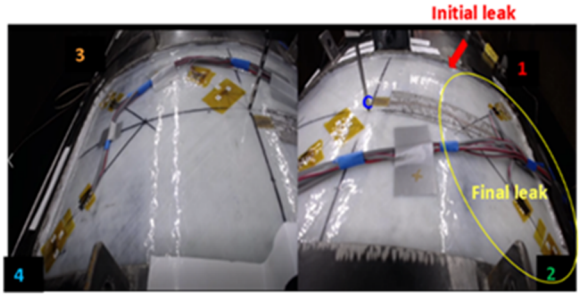

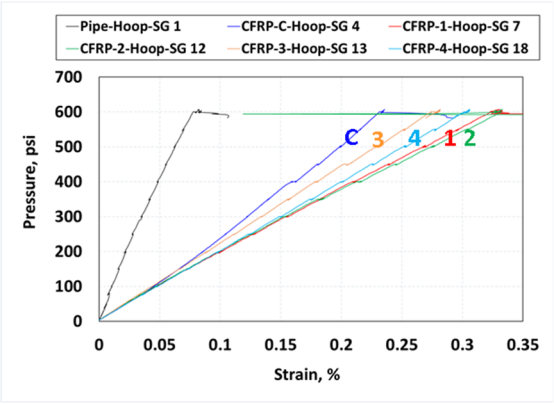

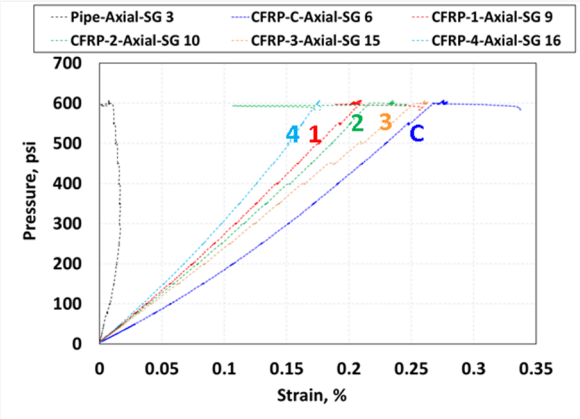

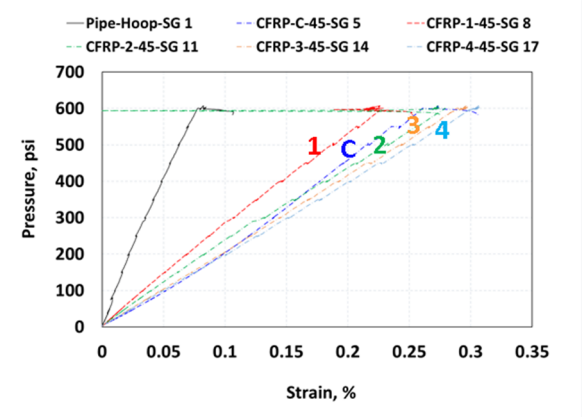

Figure 33 Strain gage data on host pipe and CFRP during the hydrostatic test

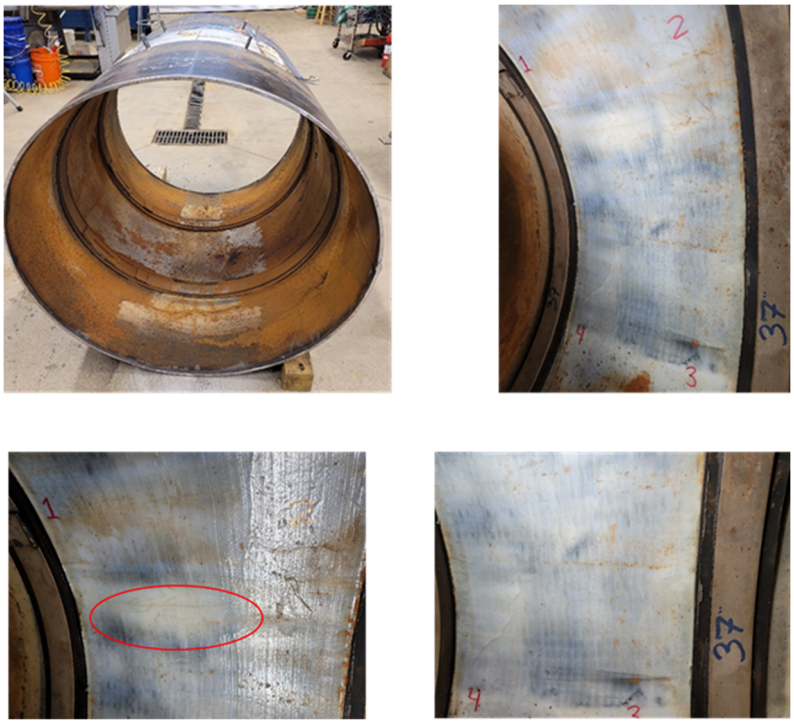

Figure 34 River-like matrix cracking on CFRP system inside the pipe after hydrostatic test

7.5 Available Margin in CFRP Repair System

After determining the failure (leak) pressure of 600 psi from the hydrostatic test, the available margin in CFRP repair system for short-term loading at room temperature (72 F) for the specified design pressure of 84 psi was calculated to be approximately 7 for leakage type of failure. *This margin of 7 confirms that the design of the CFRP repair system is conservative and the fact that the predominant failure is leakage also establishes that a typical failure is not "catastrophic" resulting in a double-ended guillotine break.* However, some key points relating to this margin should be carefully noted. The margin is determined for only short-term loading, i.e., it does not include the effect long-term use such as environmental effect and creep due to sustained loading. Also, the margin of 7 corresponds to room temperature (72 F) condition which does not include the effect of elevated temperature that the degraded pipe may experience in service condition. Another key point and probably most important is that the margin is calculated for leakage failure, not for any catastrophic failure such as rupture, fiber breakage, etc. The current workscope in this project was to design the full-scale test only to represent this baseline case. There are other parameters that could also influence the failure mode and pressure that were not addressed in this test.

7.5.1 Failure modes

The failure mode in the CFRP repair system was essentially a pinhole leak through the repair preceded by matrix cracking. Longitudinal and hoop strain data on CFRP during full-scale hydrostatic test revealed that the maximum strain in any direction at failure (leak) pressure (600 psi) was about 0.33% which is significantly lower than the tensile strain at break of about 1.5% for single-ply and multi-ply laminate (See Figure 1 and Appendix B) indicating that the matrix

cracking did not occur due to the hoop or longitudinal tensile stresses from pressure loading. It is surmised that the cracking occurred due to the longitudinal bending of CFRP system near the cut-out edges as the CFRP system bulged out through the cut-out. However, as the full-scale hydrostatic test was not conducted beyond the leak pressure (which would require very different test design), any additional margin (beyond 7) that is available for any other failure such as rupture, fiber breakage was not evaluated.

7.5.2 Effect of long-term use and elevated temperature on the available margin

This section provides a discussion on how long-term use and elevated operating or accident temperature could affect the available margin of 7 as determined for short-term loading condition above. In doing so, the environmental effect, i.e., the material adjustment factor (C), creep due to sustained loading, i.e., the time effect factor (λ) and the effect of elevated temperature need to be included. While full-scale hydrostatic tests including these factors are required to be conducted to determine the exact margin, the available coupon test results can be used to estimate the margin. Referring to Table 6, the most conservative values of C and λ for 50 years of service are 0.45 and 0.6 respectively and the preliminary results (from a related NRC project) suggest that the effect of temperature on the ultimate strength could be as low as 50%. *The combined effect of all three strength reduction factors would be about 1/8 (0.45 × 0.6 × 0.5 = 0.13) which would essentially erode this available margin of 7 entirely* Another important aspect for the service condition at elevated temperature is that the preliminary coupon tensile tests at elevated temperature (in a related NRC project) revealed that the failure mode is very different when compared to those at room temperature conditions. The tensile specimens failed in burst mode with significant matrix cracking at room temperature, whereas specimens softened and stretched at elevated temperature where they failed due to fiber breakage. This implies that the leakage type of failure due to matrix cracking observed during this full-scale test at room temperature may not be the predominant failure mode for CFRP repair system at elevated temperatures. However, this has yet to be verified.

8. SUMMARY

The current work focused on three sets of confirmatory experiments to verify the structural integrity of CFRP repair system on degraded Class 2 and 3 pipes –(i) confirmatory coupon tests to evaluate various strength reduction factors, and (ii) (ii) small-scale watertightness tests to estimate the leak pressure, and, iii) a full-scale hydrostatic test of a 40-inch diameter degraded steel pipe with CFRP repair to evaluate the available margin under short-term loading conditions at room temperature.

Several strength reduction phenomena have been identified that directly affect the effective factor of safety for the specific application of CFRP repair for nuclear Class 2 and Class 3 safety related piping such as variation in statistical analysis of ultimate strength, effect of multi-ply laminate, effect of misalignment angle, time effect factor due to sustained loading, materials adjustment factors due to harsh environmental exposure and effect of temperature. Some of these strength reduction factors have been experimentally determined in this work and their effects on the effective factor of safety for CFRP repair systems have also been discussed. The bond strength was also verified to meet the minimum bond strength requirement for a full-scale hydrostatic test.

The key findings from these coupon tests are given below.

- Values of the following strength reduction factors were determined experimentally to be as follows:
  - The strength reduction factor for the variation in statistical analysis (between characteristic value and A basis) of ultimate strength was found to be 0.84-0.89.
  - The strength reduction factor for allowable fiber misalignment in ASME BPV Code Case N-871 was found to be 0.73-0.8.
  - The Code Case N-871 recommended strength reduction factors of 0.97-0.91 for 2-4 layers of CFRP were experimentally verified and were found to be conservative (slightly non-conservative for2 layers).
- Bond strengths i.e., lap shear and pull-off strengths of CFRP repair system on both steel and aluminum-bronze substrate are higher than the minimum bond strength requirement as per CC N-871 (except one out of ten specimens on steel substrate showed lower pull-off strength than the minimum bond strength requirement)
- Since CFRP material is a new application for a safety-related nuclear application, the ASME BPV Code does not have a factor of safety (FS) recommendation. From the perspectives of nuclear safety related applications and composite materials, an *effective* factor of safety of 3.5 is deemed to be adequate for CFRP repair of Class 2 and 3 safety related piping.
- In the published version of ASME BPV CC N-871 (December 2019), a sample calculation showed that the effective factor of safety (FS_{eff}) for CFRP repair as per CC N-871 may be non-conservative (lower than the required FS_{eff} of 3.5) for 50 years of service life when the worst-case scenario of all strength reduction factors (some are experimentally determined in the project while others are recommended values in CC N-871) were included. The recommendation from the current work is that FS may need to be increased to meet the requirement or all strength reduction factors should be included in determining the strength of CFRP laminates.
- In the current version (November 2020) of CC N-871-1 (which is not approved by ASME yet) where the design section is significantly revised, some of the strength reduction factors such as time effect factor (λ), material adjustment factor (C) and effect of temperature (C_T) are included in the design calculation with a FS of 4.0 which is still calculated to be non-conservative if the rest of the strength reduction factors are included. The recommendations from the current work are that the FS needs to be increased or the remaining strength reduction factors must be included in determining the strength of CFRP laminates.

Small-scale watertightness test of the CFRP repair system is conducted using an apparatus specifically designed to conduct the hydrostatic pressurization. Per CC N-871 requirements, the watertightness test could be terminated after achieving twice the design pressure, if there is no leak. The watertightness tests in the current program were continued until the pressure dropped due to the failure of CFRP due to leakage.

The key finding from watertightness tests is given below.

- The watertightness pressures from two watertightness tests were significantly higher than the minimum requirement of twice the design pressure. The watertightness pressure for one watertightness test showed a similar failure mode (leak through the CFRP system) at 550 psi which is reasonably close to full-scale test failure (leak) pressure.

A full-scale hydrostatic test on a 40-inch diameter steel pipe with a 12-in ×24-in hole after repairing it with CFRP was conducted under short-term loading at room temperature (72 F) to evaluate the available margin. The short-term loading indicates that the CFRP repair materials have not gone through any long-term materials property degradation such as exposure to harsh environment (such as water, salt-water, etc.) or creep due to sustained loading. As the hydrostatic test was conducted at room temperature, the effect of elevated temperature was not included in this test. A pre-test finite element analysis of full-scale steel pipe with CFRP repair was performed to determine the optimal flaw (cut-out) size and shape to represent one of the design conditions for in-service piping and yet ensuring safety while conducting the test. The design calculations were conducted to determine the required configuration of CFRP layups and the CFRP repair was installed at Emc^2 laboratory.

The key points from the full-scale hydrostatic test are given below.

- As per ASME BPV CC N-871design calculations, the required number of CFRP layers was two hoop layers and one longitudinal layer for a design pressure of 84 psi at room temperature (72 F). Additionally, one dielectric and one watertightness GFRP layer were also installed. The final layup configuration is 1D+1H+1L+1W+1H.
- Overall curing and post-curing temperatures were monitored during the entire period (8 days) of CFRP installation which were within 85 F-95 F. Eight thermocouples installed at each layer of CFRP in a witness panel revealed that the curing and post-curing temperature during entire period of CFRP installation was within a tight range indicating that heat was transferred reasonably through all layers. However, it should be noted that the length of the test pipe (13-ft) and CFRP repair (2-ft) were relatively short as compared to long pipe and repair installed under field conditions.
- DSC results for the specimens from three locations from the test pipe revealed that the degree of curing for the entire CFRP repair was higher than the minimum requirement of 85%. The glass transition temperatures (T_g) for two locations from inside surface were within range of 122 F-145 F whereas the Tg at the cut-out in the outside surface was 144 F-176 F which could be due to an unintentional higher curing temperature on that location on Day 3.
- The full-scale hydrostatic test was conducted with stepwise pressure increment such that the pressure was held for at least 10 minutes for every 50-psi increment. The onset of leak started at 600 psi after about 168 minutes when a low energy water leak occurred through a small pinhole near the edge of the cut-out. After holding the pressure at 600 psi for another 40 minutes final leakage occurred with significant) cracking noise in the matrix followed by several pinhole type of leaks in the vicinity of the initial location.
- Strain gage data on CFRP system indicated that the hoop strains (which is the dominant strain) were the largest in the location near the locations of the initial and final leaks. The

strain data and cracking noise indicated that the matrix of CFRP repair system cracked potentially creating a leak path through the matrix, CFRP and GFRP watertightness layers. Post-test analysis of the inner surface of the CFRP repair system showed a lot of river-like cracking marks as well.

- There was no evidence of water found near the edge at the bond area between the host pipe and CFRP repair suggesting that the leak did not occur within the bond. No evidence of fiber breakage was noticed at 600 psi leak failure pressure.
- The available margin in CFRP repair system for short-term loading at room temperature (72 F) for this design condition (84 psi design pressure) was calculated to be slightly higher than 7 for leakage type of failure. *This margin of 7 confirms that the design of the CFRP repair system is very conservative, and the fact that the predominant failure is leakage also establishes that a typical failure is not 'catastrophic' resulting in a double-ended guillotine break.* However, this margin does not include the effect of elevated temperature and long-term use such as environmental effect and creep due to sustained loading. Also, any additional margin (beyond 7) available beyond this failure mode such as rupture or fiber breakage was not evaluated.
- Based on the strain data and failure mode, it may be surmised that the cracking occurred due to the longitudinal bending of the CFRP system near the cut-out edges as the CFRP system bulged out through the cut-out.
- The effect of long-term use and elevated operating or accident temperatures on the margin (7) under short-term loading was discussed based on the coupon test results and available data from CC N-871 to date. The preliminary estimate using the worst-case scenario showed that the available margin of 7 under short-term loading may be fully eroded under long-term and elevated temperature condition and hence, care should be taken in selecting curing temperature and the maximum allowable design temperature for any specific design and application.
- The tensile coupon specimens failed in burst mode with significant matrix cracking at room temperature whereas the specimens tested at elevated temperatures softened and stretched at elevated temperature when they failed due to fiber breakage. This implies that the leakage type of failure due to matrix cracking observed during this full-scale test at room temperature may not be the predominant failure mode for CFRP repair system at elevated temperatures.

9. Additional Considerations

While the available margin of 7 of CFRP repair under short-term loading is very conservative with a non-catastrophic leakage type failure, the effect of long-term use and elevated temperature may have a significant detrimental effect on the performance of the CFRP repair. At this time, there is insufficient data to assess the long-term degradation and performance of the CFPR repair. In addition, preliminary results have shown reduction of strength under elevated temperatures. It is therefore important to consider the performance of the CFRP repair system under long-term use such as 50 years of service with environmental effects and elevated service temperature.

Full-scale hydrostatic testes under long-term loading and elevated temperature could provide insights into:

- The predominant failure mode of the CFRP repair system at elevated temperature – leak, rupture, or debonding, and
- The available margin under long-term loading at elevated temperature considering the various failure modes.

For leak-dominant mode of failure, it would be important to better understand the capability of techniques to determine leaks. This would help establish the needed safety margin for various loading conditions.

REFERENCES

[1] ASME Boiler and Pressure Vessel Code, Section XI, Code Case N-871, "Repair of Buried Class 2 & 3 Piping Using Carbon Fiber Composite Materials", 2019.

[2] Proposed Alternative to ASME Section XI Requirements for Repair/Replacement of Circulating and Service Water Class 3 Piping in Accordance with 10 CFR 50.55a(z) (1) – Redacted – Non-proprietary Surry Power Station 2 (Unit 1 and Unit 2), (ADAMS Accession No. ML16355A346, December 14, 2016.

[3] Non-proprietary Safety Evaluation, ML17303A068, December 20, 2017.

[4] ASME Boiler and Pressure Vessel Code, Section III, 2017 Edition.

[5] American Society of Civil Engineers Standard 7-10, "Minimum Design Loads for Buildings and Other Structures", 2010.

[6] American Water Works Association (AWWA), C305 - CFRP Renewal and Strengthening of Prestressed Concrete Cylinder Pipe (PCCP, 2018.

[7] American Water Works Association (AWWA), Manual M11, Steel Pipe - A Guide for Design and Installation, Fourth Edition, 2004.

[8] American Water Works Association (AWWA), Manual M45, Fiberglass Pipe Design, Third Edition, 2013.

[9] Zarghamee, M.S., M. Engindeniz, and N. Wang, "CFRP Renewal of Prestressed Concrete Cylinder Pipe, Web Report #4352, Water Research Foundation, Denver, CO, 2013.

[10] M. Uddin, P. Krishnaswamy, C. Basavaraju and K. Manoly, "Perspectives on Safety Margin Associated with Internal Repair of Buried Class 2 And 3 Safety Related Piping Using Carbon Fiber Reinforced Polymer Composites", ASME Pressure Vessels & Piping Conference, Prague, Czech Republic, 2018.

[11] ASTM D7290-06, "Standard Practice for Evaluating Material Property Characteristic Values for Polymeric Composites for Civil Engineering Structural Applications".

[12] B. R. Ellingwood, "Toward Load and Resistance Factor Design for Fiber-Reinforced Polymer Composite Structures," ASCE Journal of Structural Engineering, Vol 129, No. 4, pp. 449-458, 2003.

[13] A. Zureick, R. M. Bennett, and B. R. Ellingwood, "Statistical Characterization of Fiber-Reinforced Polymer Composite Material Properties for Structural Design," ASCE Journal of Structural Engineering, August, Vol 132, No. 8, pp. 1320-1327, 2006.

[14] Composite Materials Handbook, "Volume 3. Polymer Matrix Composites Materials Usage, Design, and Analysis", MIL-HDBK-17-3F, 2002.

[15] Composite Materials Handbook, "Volume 1. Polymer Matrix Composites Guidelines for Characterization of Structural Materials", MIL-HDBK-17-1F, 2002.

[16] Material Qualification and Equivalency for Polymer Matrix Composite Material Systems: Updated Procedure, DOT/FAA/AR-03/19, 2003.

[17] R. Christensen and Y. Miyano, "Stress Intensity Controlled Kinetic Crack Growth and Stress History Dependent Life Prediction with Statistical Variability" International Journal of Fracture, 137: 77-87, 2006.

[18] Y. Miyano, Y., M. Nakada, and N. Sekine, 2005. Accelerated Testing for Long Term Durability of FRP for Marine Use, Journal of Composite Materials, 39(10):5-20.

[19] K. Audenaert, L. Taerwe, and D. Gazouli. 2001. Stress-Rupture of FRP: State of the Art. In Proc. of the 5th Int. Conf. on Fibre Reinforced Plastics for Reinforced Concrete Structures (FRPRCS-5), Volume 1, ed. by C.J. Burgoyne, Cambridge, 16-18 July 2001, p. 517-526

[20] Ando N., H. Matsukawa, A. Hattori, and M. Mashima. 1997. Experimental Studies on the Long-Term Tensile Properties of FRP Tendons. In Proc. of the 3rd International Symposium on Non-Metallic (FRP) Reinforcement for Concrete Structures. Sapporo, Japan.

[21] T. Yamaguchi, T. Nishimura, and T. Uomoto. 1998. Creep Rupture of FRP Rods Made of Aramid, Carbon and Glass Fibers. Structural Engineering & Construction: Tradition, Present and Future. Vol. 2; Taipei; Taiwan; 14-16 Jan. 1998. pp. 1331-1336.

[22] V. M. Karbhari, M. A. Abanilla, "Design factors, reliability, and durability prediction of wet layup carbon/epoxy used in external strengthening", Composites: Part B 38, 10–23, 2007.

[23] M. A. Abanilla, Y. Li, V. M. Karbhari, "Durability characterization of wet layup graphite/epoxy composites used in external strengthening", Composites: Part B 37, 200–212, 2006.

[24] V. M. Karbhari, K. Ghosh, "Comparative durability evaluation of ambient temperature cured externally bonded CFRP and GFRP composite systems for repair of bridges", Composites: Part A 40, 1353–1363, 2009.

[25] M. A. Abanilla, V. M. Karbhari, Y. Li, "Interlaminar and intralaminar durability characterization of wet layup carbon/epoxy used in external strengthening", Composites: Part B 37, 650–661, 2006.

[26] M. Uddin, S. Pothana and P. Krishnaswamy, "Overview of Limited Confirmatory Testing Program on Carbon Fiber Reinforced Plastic (CFRP) Repair System at Emc^2", NRC Public Meeting, Composite Repair Technical Information Exchange, ML20014E579, 2020.

[27] Xinbao Yang, Antonio Nanni, Stephen Haug, and Chung Leung Sun, "Strength and Modulus Degradation of CFRP Laminates from Fiber Misalignment", Journal of Materials in Civil Engineering, Vol. 14, Issue 4, 2002.

[28] F. Rodriguez, "Principles of Polymer Systems", 2nd Edition, 1982.

[29] R. J. C. Carbas, E. A. S. Marques, L. F. M. Da Silva, and A. M. Lopes, "Effect of Cure Temperature on the Glass Transition Temperature and Mechanical Properties of Epoxy Adhesives", The Journal of Adhesion, 90:104–119, 2014.

[30] Sinclair, J W, "Effects of Cure Temperature on Epoxy Resin Properties", The Journal of Adhesion, Volume 38, 1992.

[31] T.J. Varley, J. H. Hodgkin, and G. P. Simon, "Toughening of Trifunctional Epoxy System. V. Structure – Property Relationships of Neat Resin, Journal of Applied Polymer Science 77, 237 – 248, 2000.

[32] J. B. Enns and J. K. Gillham, "Effect of the Extent of Cure on the Modulus, Glass Transition, Water Absorption, and Density of An Amine-Cured Epoxy", Journal of Applied Polymer Science 28, 2831 – 2846, 1983.

[33] S. Ziaee, and G. R. Palmese, "Effects of Temperature on Cure Kinetics and Mechanical Properties of Vinyl–Ester Resins", Journal of Polymer Science: Part B: Polymer Physics 37, 725 – 744, 1999.

[34] P. Li, X. Yang, Y. Yu, and D. Yu, "Cure Kinetics, Microheterogeneity, and Mechanical Properties of the High-Temperature Cure of Vinyl Ester Resins", Journal of Applied Polymer Science 92, 1124 – 1133, 2004.

[35] ASME Boiler and Pressure Vessel Code, Section VIII, Division 1, 2017 Edition.

[36] J. W. Baur, D. J. Hartl, G. J. Frank, R. Bradford, G. Huff, "Graphical material selection methods for multi-constraint, multi-functional composites Pressure Vessels", ASME Pressure Vessel and Piping Conference, PVP2017, Hawaii, 2017.